Zeta Potential of Intact Natural Limestone: Impact of Potential-Determining Ions Ca, Mg and SO_4

A. Alroudhan[1], J. Vinogradov[1], and M.D. Jackson[1]

[1]Department of Earth Science and Engineering, Imperial College London SW7 2AZ

Corresponding Author: Abdulkareem Alroudhan – a.alroudhan11@imperial.ac.uk

Colloids and Surfaces A: Physicochem. Eng. Aspects 494 (2016) 83-90, doi: 10.1016/j.colsurfa.2015.11.068

Abstract

We report measurements of the zeta potential on intact limestone samples obtained using the streaming potential method (SPM), supplemented by the more ubiquitous electrophoretic mobility method (EPM). The effect of the potential-determining ions (PDI) Ca, Mg and SO_4, and the total ionic strength controlled by NaCl concentration, is investigated over the range typical of natural brines. We find that the zeta potential varies identically and linearly with calcium and magnesium concentration expressed as pCa or pMg. The zeta potential also varies linearly with pSO_4. The sensitivity of the zeta potential to PDI concentration, and the IEP expressed as pCa or pMg, both decrease with increasing NaCl concentration. We report considerably lower values of IEP than most previous studies, and the first observed IEP expressed as pMg. The sensitivity of the zeta potential to PDI concentration is lower when measured using the SPM compared to the EPM, owing to the differing location of the shear

plane at which the zeta potential is defined. SPM measurements are more appropriate in natural porous samples because they reflect the mineral surfaces that predominantly interact with the adjacent fluids. We demonstrate that special cleaning procedures are required to return samples to a pristine zeta potential after exposure to PDIs. We apply our results to an engineering process: the use of modified injection brine composition to increase oil recovery from carbonate reservoirs. We find a correlation between an increasingly negative zeta potential and increased oil recovery.

Introduction

The zeta potential of natural carbonates plays a role in many subsurface processes, governing the electrostatic interactions between mineral surfaces and polar species in both aqueous and non-aqueous phase liquids (NAPLs). For example, the self-freshening often observed when brackish water invades a freshwater aquifer depends on preferential adsorption of aqueous salt species such as Ca and Mg (e.g. Appelo, 1994), while contaminated carbonate aquifers may be remediated through sequestration of the contaminant by co-precipitation with the mineral phase (Meece and Benninger, 1993). Uptake of contaminants such as heavy metals is related to their reactivity as a function of the ionic strength and pH of the aqueous electrolyte (Reeder et al., 2001). The wetting state of carbonate oil reservoirs is believed to be influenced by the zeta potential (Buckley et al., 1998; Gomari et al., 2006), as is the success of enhanced oil recovery by modification of injection brine composition and/or ionic strength (Zhang and Austad, 2006; Yousef et al., 2010). Moreover, solubility of CO_2 in brine as a trapping mechanism in saline aquifers is an important component of carbon capture and storage (Riley, 2010). Compared to sandstones, aqueous CO_2 solubility is greatly enhanced in the presence of carbonate minerals such as calcite (Rosenbauer et al., 2005). The increase in CO_2 concentration has a profound

effect on pH (Pokrovsky et al., 2005), which in turn alters the zeta potential of calcite and leads to its dissolution (Eriksson et al., 2007). The zeta potential is also an important control on the use of self-potential measurements to monitor subsurface fluid flow (e.g. Saunders et al. 2008; Gulamali et al., 2011; Jackson et al., 2012a, b).

The calcite-water interface is electrically charged with the calcite crystal lattice constituents Ca^{2+} and CO_3^{2-} being the main potential determining ions (PDIs, being those ions whose concentration in aqueous solution controls the polarity and density of electrical charge on the mineral surface; Somasundaran and Agar, 1967). However, it is well known that divalent ions such as Mg^{2+} and SO_4^{2-} are also PDIs (Pierre et al., 1990). Figure 1 shows that there are numerous papers reporting measurements of the zeta potential on calcite. The zeta potential is modified by the concentration of both indifferent and potential-determining ions, with the concentration of indifferent ions controlling the thickness of the electrical double layer, and the concentration of PDIs controlling both the double layer thickness and the mineral surface charge. Previous studies of the zeta potential on calcite have highlighted the difference between natural and artificial calcite samples (e.g. Cicerone et al., 1992, Vdovic, 2001), the importance of controlling CO_2 partial pressure (pCO_2) in open or closed-system experiments (Thompson and Pownall, 1989; Heberling et al., 2011), the impact of wetting state in the presence of NAPLs (e.g. Jackson and Vinogradov, 2012; Kasha et al., 2015), and the effect of PDI concentration (Pierre et al., 1990; Zhang and Austad, 2006; Strand et al., 2006; Alotaibi et al., 2011; Chen et al., 2014; Alotaibi and Yousef, 2015; Mahani et al., 2015a,b). However, few report measurements of zeta potential in carbonates at conditions relevant to natural subsurface systems. Most explore only dilute electrolytes, with much lower total ionic strength and PDI concentration than subsurface brines, and crushed rather than intact rock samples. Moreover, most do not employ an experimental method that establishes equilibrium conditions of pH, pCO_2 and PDI concentration relevant to subsurface carbonates. Many use artificial calcite,

open system measurements with uncontrolled pCO_2, or vary pH and/or pCO_2 over a broad range not relevant to subsurface brines.

Most previous studies utilised measurements of electrophoretic mobility (EPM) to determine the zeta potential (Madsen, 2002). In this approach, the sample is crushed to a fine powder and suspended in a solution of the electrolyte of interest. An electrical potential field is applied across the suspension (the field typically oscillates at a controlled frequency, inducing an alternating current through the suspension) and the resulting movement of the solid particles is used to interpret the zeta potential via the Helmholtz-Smoluchowski equation (see Delgado et al., 2007). EPM measurements may not reflect the natural conditions of interest for several reasons. First, the samples are crushed, which creates 'fresh' mineral surfaces that may have different properties to 'aged' surfaces that have been previously exposed to fluids in the pore-space. Second, the ratio of electrolyte volume to mineral surface area is significantly changed compared to the natural porous medium, which may be important in systems such as carbonates where dissolution and precipitation and/or adsorption and desorption may simultaneously modify surface charge and electrolyte composition (Thompson and Pownall, 1989; Pierre et al., 1990). Third, the EPM method is limited to representing only one solid or fluid phase in addition to the supporting electrolyte. Hence, it cannot be used to obtain multiphase measurements when both NAPLs and water are present within the rock pore-space, as is often the case in subsurface carbonates.

The aim of this study is to determine the zeta potential in *intact* natural carbonate samples saturated with aqueous electrolytes containing PDIs at similar concentration to natural brines, and with total ionic strength similar to natural brines. We are particularly interested in determining how the zeta potential is affected by the concentration of PDIs such as Ca, Mg and SO_4 over the range found in natural brines. Several previous studies have investigated the relationship between Ca concentration and zeta potential, but these typically probed

concentration ranges much lower than natural brines (e.g. Foxall et al., 1978; Thompson and Pownall, 1989; Pierre et al., 1990; Cicerone et al., 1992). Much less attention has been paid to the role of Mg and SO_4 as PDIs yet these ions are also abundant in natural brines such as seawater (e.g. Zhang and Austad, 2006;). We also wish to determine how the zeta potential is affected by the concentration of these PDIs in the presence of Na and Cl ions over the range found in natural brines. Na and Cl are by far the most common ionic species found in such brines and are believed to be indifferent to the calcite mineral surface; nonetheless, it has not yet been determined whether the effect of the known PDIs (Ca, Mg and SO_4) on carbonate surface charge is modified by the presence of Na and Cl at high concentration.

Rather than the EPM used in most previous studies, we used the streaming potential method (SPM) described by Jackson and Vinogradov and co-workers (Jaafar et al., 2009; Vinogradov et al., 2010; Vinogradov and Jackson, 2011; Jackson and Vinogradov, 2012). The advantage of the SPM is that it can be used with intact samples, including the cylindrical core plugs that are ubiquitously obtained from subsurface reservoirs (Jaafar et al., 2009), is suitable for high ionic strength (>2M, where M represents moles/litre) electrolytes (Vinogradov et al., 2010), can be used to measure zeta potential during multiphase flow and for varying wettability (Vinogradov and Jackson, 2011; Jackson and Vinogradov, 2012), and can be extended to the elevated temperatures (up to 150^{o}C) often found in deep saline aquifers, hydrocarbon reservoirs, and geothermal systems (Vinogradov and Jackson, 2015). The SPM measurements were complemented by pH and electrical conductivity measurements, and chemical analysis of the effluent electrolyte, to ensure accuracy of the reported compositions and monitor any adsorption/desorption and/or dissolution/precipitation that occurred during the experiments. In addition, we report zeta potential measurements using EPM for the same materials (rock and electrolytes) and preparation procedure, which allows direct comparison between these two electrokinetic methods.

Our approach contrasts with many previous studies because the experimental method is specifically designed to ensure the equilibrium achieved between sample and electrolyte is consistent with natural processes. The results are directly applicable to a wide variety of natural subsurface carbonates. Here we apply our results to a key engineering process relevant to subsurface carbonates: the use of modified injection brine composition to increase oil recovery in a process termed controlled salinity waterflooding (CSW).

Methodology

Materials and sample preparation

The rock samples used in the experiments are Portland limestone from the Portland quarry on the south coast of the UK (Table 1). We used two different types of electrolyte. The first comprised reagent-grade NaCl, $CaCl_2.2H_2O$, Na_2SO_4 (Sigma-Aldrich), $MgCl_2.6H_2O$ (Fluka Analytical) solutions in deionized water (DIW) from a Thermo Scientific filtered system with electrical conductivity below 1 μS/cm. In these electrolytes, the maximum concentration probed was 2M for NaCl, 0.42M for $CaCl_2$ and $MgCl_2$, and 0.13M for Na_2SO_4. The second comprises natural seawater (SW) from the Arabian Gulf, collected from Dammam, Saudi Arabia. The natural seawater sample was treated with UV light and then filtered through 5 μm filter paper. Table 2 lists the compositions of the electrolytes used, including the natural seawater and synthetic formation brine (FMB) typical of oil reservoirs and deep saline aquifers (e.g. Romanuka et al., 2012).

The majority of limestone formations are directly deposited in seawater (Morse, 1986; Morse and Mackenzie, 1990) and the seawater is in equilibrium with both calcite and CO_2 (Stumm and Morgan, 1996). Any factor, such as organic activity, CO_2 partial pressure, or temperature that modifies the equilibrium will result in precipitation or dissolution of calcite. Carbonate minerals are soluble in water and dissolution yields carbonate ions (CO_3) that can react to form bicarbonate (HCO_3) and hydroxide (OH) ions according to the equilibrium reaction

$$CaCO_{3\,(s)} \leftrightarrow Ca^{2+} + CO_3^{2-}$$
$$CO_3^{2-} + H_2O \leftrightarrow HCO_3^{-} + OH^{-} \quad (1)$$

If the system is open, atmospheric CO_2 dissolves into the water, reacting directly with hydroxide to form bicarbonate and hence reducing the pH according to the equilibrium reaction

$$CO_{2(aq)} + OH^{-} \leftrightarrow HCO_3^{-} \quad (2)$$

Equilibrium between calcite and water in the presence of CO_2 is reached when most of the carbonate ions are turned into bicarbonate (Krauskopf, 1989); this corresponds to a minimum aqueous concentration of carbonate and carbonic acid, and a maximum for bicarbonate (Figure 2b). The equilibrium is affected by the total ionic strength, including the concentration of Na and Cl ions that are often found in natural brines. In simple solutions of $CaCO_3$ exposed to CO_2 at 25^{o}C the equilibrium pH is 8.3-8.4 (Garrels and Christ, 1965, Stumm and Morgan, 1996; Figure 2a).

These conditions of carbonate/water/CO_2 equilibrium were replicated here using the following two-stage equilibration procedure. For DIW-based electrolytes, we began by preparing a NaCl solution of the desired concentration in DIW. In the first stage of the equilibration procedure, this solution was placed in a beaker with offcuts of the Portland limestone, maintaining an air layer in the beaker to provide a source of atmospheric CO_2 but sealing the beaker to prevent

evaporation. Monitoring of the pH (using a Five-Go Mettler-Toledo pH meter with their 3-in-1 pH electrode LE438, implementing where necessary the manufacturer's recommended calibration and correction procedures at high ionic strength) and Ca concentration (described below) confirmed the dissolution of calcite and associated pH changes discussed above (e.g. Figure 2b). The initial increase in pH reflects the formation of hydroxide ions according to the equilibrium reaction (1). The subsequent decrease in pH reflects the formation of bicarbonate according to the equilibrium reaction (2). In this case the final pH of the equilibrated solution was c. 8.2, consistent with the predicted value for a simple open system $CaCO_3$ solution (Figure 2a). Dissolution of calcite is demonstrated by the increase in Ca concentration from zero to approximately 0.001±0.0001 M (Figure 2a). The resulting equilibrated NaCl solution was termed NaCl-EQ, and this first stage of equilibration mimics the open-system conditions when the carbonate sediments are first deposited. For the experiments reported below, equilibrated solutions of three different NaCl concentrations (0.05M, 0.5M, and 2M) were prepared. Equilibrium was assumed to have been reached when the measured change in both pH and pCa (where p represents the negative logarithm) was zero within experimental error over a timespan >350 hours (two weeks). The equilibrium pH was found to be consistently 8.2±0.2 for 0.05M and 0.5M NaCl electrolytes, and 8.3±0.3 for 2M NaCl electrolyte. The NaCl-EQ solution was then used directly in zeta potential measurements, or was modified by addition of PDIs. This first stage of the equilibration procedure is essential to ensure equilibrium between calcite, water and atmospheric CO_2 and prevent calcite dissolution and associated changes in surface charge during measurements of zeta potential.

The core flooding apparatus used to measure the zeta potential in the SPM (described below) is closed to the atmosphere, and the second stage of equilibration prior to measuring the zeta potential was to ensure equilibrium between the electrolyte of interest (NaCl-EQ after the addition of any PDIs to be studied) and the rock sample at the closed-system conditions

pertaining to a rock-brine system at depth. The rock sample was pre-saturated with the selected electrolyte at open-system conditions and then confined in the core holder at closed-system conditions, and the electrolyte was pumped through the sample from the (closed) inlet reservoir to the (closed) outlet reservoir and back again. The repeated flow of the electrolyte through the sample at closed system conditions mimics migration of the electrolyte into the carbonate rock at depth. At regular intervals, the electrical conductivity and pH of the electrolyte in the reservoirs was measured, and equilibrium was assumed to have been reached when the conductivity and pH of the electrolyte in each reservoir differed by <5%. The pH varied over a small range in all experiments and was consistent with reported values for natural brines in carbonate rocks (pH in the range 7-8; Yousef et al., 2012). Addition of Ca or Mg reduced the pH to the range 7.2-8, while addition of SO_4 caused a smaller change, yielding pH in the range 7.9-8.1. The uncertainty in the measured values of pH was always less than ±0.3.

Prior to a given experiment, the rock sample was cleaned in a Soxhlet apparatus with methanol for 48 hours. It was then dried for at least 12 hours in a vacuum oven at 80^{o}C. Then, it was allowed to cool at room temperature for a minimum of 6 hours. This is a standard core sample cleaning procedure used in many previous studies and was used with fresh samples here (e.g., Jaafar et al., 2009). However, for reasons discussed later in the paper, after a series of experiments using electrolytes with elevated PDI concentration, the rock samples were flooded with at least 2 pore-volumes (PV) of deionized water (DIW) prior to the methanol cleaning step, and were then flooded with a further 4 PV of 0.05M NaCl-EQ electrolyte. The conductivity of the effluent electrolyte was measured in order to confirm it was the same as that obtained on the fresh samples using the same electrolyte within a 5% tolerance.

For comparison, the zeta potential of one selected sample was also measured using the EPM method (described below). Off-cuts of fresh Portland Limestone were cleaned for 48 hours in methanol and then crushed using a jaw crusher. A Tema Mill with an agate vessel was then

used to obtain a fine powder of the sample. NaCl-EQ was used to prepare solutions with different Ca content. Suspensions of 0.05g of Portland powder in 50mL (1 wt. %) of the desired electrolyte were prepared and left for a minimum of 1 hour, to allow the fraction of larger suspended particles to settle out of solution. For each sample, the suspension was injected via a syringe into a capillary cell in order to obtain the zeta potential measurement. Care was taken to ensure no air bubbles were left in the cells.

Measurement of Zeta Potential

Streaming Potential Measurement (SPM)

The zeta potential was measured using the SPM described by Vinogradov et al. (2010). Only a brief summary of the method is provided here. The carbonate core samples were tightly confined within an embedded rubber sleeve in a stainless steel core holder with non-metallic end caps. A syringe pump was used to induce a fluid pressure difference across the sample, causing the electrolyte to flow through the sample from reservoirs connected to each side of the core holder (Figure 3). Synthetic oil was used to translate the induced pressure from the pump to the brine in the inlet reservoir, which maintains closed-system conditions by preventing exposure of the electrolyte to atmosphere. The pump maintains constant rate to high accuracy and flow can be directed in either direction through the sample.

The pressure difference across the sample was measured using a pair of pressure transducers (calibrated Druck PDCR 810 with accuracy 0.1% of measured value, resolution 70 Pa) and the voltage across the sample was measured using non-polarizing Ag/AgCl electrodes and an NI9219 voltmeter (internal impedance >1GΩ, accuracy 0.18%, resolution 50 nV). The noise level of the measurements is dictated by the stability of the electrodes, rather than the performance of the voltmeter. The electrodes were positioned out of the flow path, in an

electrolyte reservoir of a NaCl solution of the same ionic strength as that used in the experiments.

We used the 'paired-stabilization' or PS method of Vinogradov et al. (2010) to measure the streaming potential across the sample, in which flow is induced through the sample at the same rate but in opposing directions. The method eliminates the effect of temporal variations in the static voltage and demonstrates that electrode polarization effects are negligible through confirmation that the change in potential induced by flow in one direction is equal and opposite to the change in potential induced by flow in the opposite direction. To ensure that exclusion-diffusion potentials were eliminated during measurements of the streaming potential, uniform and constant electrolyte conductivity and pH in each reservoir, and uniform and constant temperature (23°C), were maintained within a 5% tolerance. Redox potentials, which may affect the measured voltage if metals such as steel are in contact with the saline electrolyte, were eliminated by electrically isolating all metallic components from the electrolyte except for the Ag/AgCl electrodes.

Interpretation of the results from the PS experiments follows from the observation that at steady-state, the streaming current induced by the flow is balanced by a conduction current to maintain overall electrical neutrality. It is reasonable to assume that the currents follow approximately the same 1-D path along the samples, in which case the streaming potential coupling coefficient can be determined using

$$C_{SPM} = \frac{\Delta V}{\Delta P} \tag{3}$$

where ΔV and ΔP are the stabilized voltage and pressure measured across the plug, respectively. The coupling coefficient is given by the slope of a linear regression through a plot of voltage against pressure difference obtained for a number of different flow rates (e.g. Figure 4c, d). An effective value for the zeta potential for the sample was obtained using a

modified version of the Helmholtz-Smoluchowski equation that accounts for surface electrical conductivity (e.g. Jackson, 2015)

$$\zeta = \frac{C_{SPM}\mu\sigma_{rw}F}{\varepsilon} \quad (4)$$

where F is the formation factor, which is the ratio of the conductivity of the electrolyte to the conductivity of the saturated rock sample when surface conductivity is negligible (e.g. Jouniaux and Pozzi, 1995), ε is the permittivity of the electrolyte, μ is the electrolyte viscosity and σ_{rw} is the electrical conductivity of the saturated rock sample. The formation factor and electrical conductivity were measured following the methodology of Vinogradov et al. (2010) (Table 1). Note that the zeta potential obtained is an effective value because it reflects the average streaming charge density transported by the flow of the electrolyte; at the pore-level, the zeta potential may vary. The viscosity and permittivity of the electrolyte as a function of ionic strength were also determined using the approach of Vinogradov et al. (2010). Uncertainty in the reported value of zeta potential reflects the range of possible regressions that can be fitted to the measured streaming potential data within experimental error (Figure 4).

Electrophoretic Mobility Measurement (EPM)

The zeta potential for one powdered sample in suspension was also obtained for comparison with the SPM using a Brookhaven ZetaPALS zetameter to measure the electrophoretic mobility u_e of the suspension; this is related to the zeta (shear plane) potential using the Helmholtz-Smoluchowski equation for electrophoresis (Delgado et al, 2007):

$$\zeta = \frac{u_e\mu}{\varepsilon} \quad (5)$$

As noted above, the zeta potential obtained is an effective value because it reflects the average surface charge on the particles in suspension; at the particle level, the zeta potential may vary. The measurement of each sample consisted of 5 runs; each run consisted of 10 cycles. The

mean of all the runs for each sample is reported as the zeta potential and the error bars represent the standard deviation.

Measurement of Electrolyte Composition

Electrolyte composition was determined using inductively coupled plasma atomic emission spectroscopy (ICP-AES). The analysis was carried out in the Analytical Chemistry Laboratory at the Natural History Museum, London.

Electrolyte samples from the SPM measurements were collected from the core holder via a valve on the outlet flow line at the end of a given suite of zeta potential measurements for the chosen electrolyte; each effluent sample had therefore interacted with the rock sample for a minimum volume of 10 PV spread over a minimum of two days. These samples are referred to as the final effluent electrolytes. Appropriate dilutions were prepared for each sample prior to analysis depending on the total ionic strength and relative abundance of the PDIs of interest. All samples were acidified with 2% HNO_3 to prevent formation of complexes that might affect the interpreted concentrations.

Reference standard solutions at concentrations ranging from 0.5 - 200 ppm containing all the ions of interest (Na, Ca, Mg, and S) were prepared to represent the ion matrix of the effluent samples. The accuracy of the method was determined using certified check solutions and the repeatability by conducting 5 repeat measurements on all the samples whose standard deviation is represented by the error bars.

Design of Experiments

In this work, we investigated the effect of three key PDIs (Ca, Mg and SO_4) on the zeta potential of natural limestone in two ways. The first approach was to systematically vary the concentration of each PDI over the range found in natural brines to establish its effect on the zeta potential. For each range of PDI concentrations, we tested three different NaCl (0.05M,

0.5M and 2M) concentrations to determine whether this changes the relationship between the PDI concentration and surface charge. The 0.5M NaCl concentration represents seawater and is similar to the 'ZP brine' of Zhang and Austad (2006) and Zhang et al. (2007) which contained 0.573M NaCl, allowing direct comparison of results. The 0.05M NaCl concentration represents a tenfold dilution of seawater and approximates the injection brine used in controlled salinity waterflooding (CSW) for enhanced oil recovery (Yousef et al, 2010), while the 2M NaCl concentration represents the saline brines found in many deep saline aquifers. The second approach was to combine all three PDIs in the proportions and total concentration typical of (i) natural saline brines, and (ii) natural seawater, and compositions derived from seawater similar to those used in CSW.

Results

Measurements of streaming potential and interpretation of zeta potential

Figure 4(a, b) shows typical results for the PS experiments for low and high ionic strength electrolytes respectively. The pressure response to pumping is clear and the pressure difference across the samples reached a stable value (fluctuations <500 Pa around an induced pressure difference of c. 500kPa) in all experiments. The voltage response is also clear and reached a stable value with fluctuations typically below ±5μV at high ionic strength (e.g., FMB) and below ±50μV at low ionic strength (<0.5M NaCl) in all experiments. The interpreted values of stabilized pressure and voltage are denoted by the dashed lines, while the error bars show the interpreted spread. The stabilized voltage was reproducible within ±25μV across three repeat experiments at a given flow rate for high ionic strength and ±35μV for low ionic strength. The voltage fluctuations, and reproducibility of the stabilized voltage measurements, are similar to previous experiments conducted on limestone samples saturated with electrolytes of similar

ionic strength (Jackson and Vinogradov, 2012). An important aspect of the SPM is that the polarity of the surface charge is very clear: if the polarity of the voltage response is in the opposite sense to the pressure response (i.e. a more positive pressure difference yields a more negative voltage difference relative to a common reference pressure and voltage at one end of the sample) then the surfaces are negatively charged, and vice-versa. This allows the iso-electric point (IEP) to be accurately determined even when the zeta potential is close to zero.

Figure 4 (c, d) shows typical plots of the stabilized voltage plotted against the corresponding stabilized pressure difference from each pair of PS experiments for the same electrolytes shown in Figs (a, b) respectively. The error bars represent the reproducibility of (typically) three repeat measurements at each flow rate. The streaming potential coupling coefficient, obtained from a linear regression through the measured data (equation 3), is clearly negative in Fig 4c and positive in Fig. 4d and the linear regression is well constrained by the relatively small error bars associated with each value of stabilized voltage (Fig. 4a,b). We calculate the associated zeta potential using equation (4). The uncertainty in the streaming potential coupling coefficient arising from the range of linear regressions that can be forced through the stabilized voltage and pressure data was used to determine the associated uncertainty in zeta potential reported in the following sections.

Impact of Ca, Mg and SO_4 concentration on zeta potential

We begin by reporting experiments in which the concentration of each PDI was systematically varied in pre-equilibrated 0.05M NaCl electrolytes (NaCl-EQ). Figure 5 shows the zeta potential as a function of calcium, magnesium and sulfate concentration. We plot concentration as pPDI. Note that in all cases the lowest concentration (highest pPDI) investigated corresponds to the equilibrated concentration in the NaCl-EQ electrolyte. We notice first that a linear regression provides an excellent fit to the data for each PDI (R^2 >0.98) and that the gradient of the regression for Ca and Mg is identical within experimental error (-5.10 ± 0.47 mV/decade).

Moreover, the zeta potential is negative at high pCa or pMg (i.e. low Ca or Mg concentration), becomes less negative with decreasing pCa or pMg, and becomes positive at low pCa or pMg. The IEP (defined as pPDI) is identical for Ca and Mg (pPDI = 0.60±0.03) within experimental error. However, the behaviour of SO_4 is very different. The zeta potential remains negative regardless of pSO_4 and becomes increasingly negative with decreasing pSO_4 (i.e. increasing SO_4 concentration). Moreover, the gradient of the linear regression that best fits the data is much smaller than that observed for Ca and Mg (1.9 ±0.3 mV/decade). These results suggest that Ca and Mg behave almost identically as PDIs at room temperature and can have a significant impact on zeta potential, yielding positive zeta potential at pPDI < 0.60. However, the zeta potential is much less sensitive to pSO_4.

Impact of varying the concentration of NaCl

Figure 6 shows the zeta potential as a function of Ca concentration for each of the three NaCl concentrations investigated (Figure 6a), and as a function of SO_4 concentration for two of the NaCl concentrations investigated (Figure 6b). Considering first the impact of Ca concentration, we again find that a linear regression provides an excellent fit to the data for each value of NaCl concentration ($R^2 > 0.98$) and that the gradient of the linear regression decreases with increasing NaCl concentration (Figure 6c). Thus, the zeta potential becomes less sensitive to pCa as the NaCl concentration increases. In all cases, the zeta potential is negative at high pCa (i.e. low Ca concentration), becomes less negative with decreasing pCa, and becomes positive at low pCa. The IEP (defined as pCa) decreases with increasing NaCl concentration although the change only exceeds experimental error for the lowest NaCl concentration investigated (Figure 6c). Considering next the impact of SO_4 concentration, we observe similar behaviour. A linear regression again provides an excellent fit to the data, and the gradient of the regression decreases with increasing NaCl concentration (Figure 6b). However, the zeta potential remains negative over the range of pSO_4 investigated.

Effect of varying multiple PDIs

In this section, we report measurements of zeta potential using electrolytes containing all three PDIs (Ca, Mg, and SO_4) at the concentrations found in typical formation brine (FMB; Table 2) and seawater (SW; Table 2). The formation brine yields a positive zeta potential, which is the same within experimental error as the zeta potential obtained by adding a comparable amount of Ca to 2M NaCl electrolyte (see the filled square in Fig. 5). The natural seawater yields a negative zeta potential, which is more negative than the zeta potential obtained by adding a comparable amount of Ca to 0.05M NaCl electrolyte (see the open square in Fig. 5). Thus the zeta potential in subsurface saline brine appears to be controlled primarily by the Ca content, with Mg and SO_4 playing a minor role; in contrast, the presence of SO_4 in seawater leads to a more negative zeta potential.

We also investigate the effect of diluting seawater and adding SO_4 to seawater. Both of these approaches to modifying the brine injected into carbonate oil reservoirs have been suggested to yield enhanced oil recovery (Zhang and Austad, 2006; Yousef et al. 2011). In the experiments conducted here, seawater (SW) was diluted twice (1/2SW), ten times (1/10SW) and twenty times (1/20SW), and SO_4 was added to yield twice (2SW), three times (3SW) and four times (4SW) the natural seawater concentration. In all cases, the measured zeta potential is negative (Figure 7a); however, the least negative (or smallest in magnitude) zeta potential is observed for seawater, and the zeta potential becomes increasingly negative (and larger in magnitude) as the seawater is diluted or SO_4 is added. The zeta potential increases in magnitude with both increasing and decreasing total ionic strength (Figure 7b); the ionic strength increases as SO_4 is added, but decreases as the seawater is diluted.

Effect of sample preparation

Many experimental studies use a limited number of samples that are cleaned before each experiment. However, none have confirmed that the typical laboratory cleaning protocol

(described here in the methodology) restores the zeta potential of natural carbonates to a consistent and repeatable value for a given electrolyte. To confirm the repeatability of zeta potential measurements obtained using the SPM, and determine the effect of sample cleaning, the zeta potential for three selected fresh samples was initially measured using 0.05M NaCl-EQ electrolyte (circles in Fig. 8). The samples were then used in experiments in which the Ca or Mg concentration was increased (triangles in Fig. 8; these data are also shown in Fig. 5). The samples were then cleaned using a standard laboratory cleaning protocol and the zeta potential was measured again (diamonds in Fig. 8). Finally the samples were cleaned using the enhanced cleaning protocol reported here (squares in Fig. 8). It is clear that the standard cleaning procedure fails to return pMe (representing the Ca + Mg concentration) or zeta potential to their original fresh values after the samples are exposed to elevated PDI concentrations. It is important to use the enhanced cleaning procedure reported here to flush PDIs from the mineral surfaces and return the zeta potential to its pristine value.

Discussion

Comparison with previous studies of the effect of PDI concentration on zeta potential in natural and synthetic calcite/carbonates

We have demonstrated here that Ca and Mg change the zeta potential of intact natural limestone samples, causing a linear decrease in the magnitude of the negative zeta potential with increasing concentration (expressed as pPDI), and causing polarity inversion to positive zeta potential at high concentration; moreover, the two PDIs behave identically within experimental error. Similarly, SO_4 changes the zeta potential of natural limestone, causing a linear increase in the magnitude of the negative zeta potential with increasing concentration (expressed as pPDI), but the gradient of the linear regression that best fits the data is lower than that of the cations. We have also demonstrated that the gradient of the zeta potential with respect to pCa

and pSO_4 decreases with increasing NaCl concentration. The relationship between zeta potential and pPDI is linear across the entire range of pPDI investigated.

No previous studies have determined the relationship between zeta potential and pMg, but several have reported a linear relationship between zeta potential (or its proxy, electrophoretic mobility) and pCa as observed here (e.g. Foxall et al., 1979; Thompson and Pownall, 1989; Pierre et al. 1990). However, these studies were conducted using electrolytes of much lower ionic strength than those considered here (e.g. Fig. 9a). Other studies have observed a non-linear relationship between zeta potential and pCa (e.g. Cicerone et al. 1992; Chen et al., 2014). Linear behaviour is expected if the calcite surface behaviour is Nernstian and the lattice ions Ca and CO_3 are the PDIs, and the electrical double layer is described by the Gouy-Chapman-Grahame model (e.g. Hunter, 1981). Under these circumstances, the gradient of the zeta potential with respect to pPDI can be expressed as (e.g. Foxall et al., 1979)

$$\left.\frac{d\zeta}{dpPDI}\right|_{\zeta\to 0} = \frac{-2.303\frac{kT}{ze}}{\left(1+\frac{C_d}{C_s}\right)\exp(\kappa\Delta)} \qquad (5)$$

where k is Boltzmann's constant, T is the temperature, z is the valence of the PDI, e is the charge on an electron, C_d and C_s are the capacitance per unit area of the diffuse and Stern layers respectively, κ is the inverse Debye length, and Δ is the distance of the shear plane from the Stern plane. For low zeta potential, C_d is given approximately by $\kappa\varepsilon$ where ε is the permittivity. Cicerone et al. (1992) argued that the relationship between zeta potential and pPDI is linear only close to the IEP; away from the IEP, zeta potential values level off, because the Stern layer capacitance C_s varies, or because the Gouy-Chapman-Grahame model breaks down. We

do not observe this levelling off, despite the broad range of pCa values investigated. Equation 5 can be used to fit our experimental data for pCa (and pMg). However, the decrease in gradient with increasing NaCl concentration can only be matched by adjusting the Stern capacitance (see Table 3; these values are discussed in more detail in the next section). Large values of Stern capacitance are required in the range 1.13-2.75 Fm^{-2}, which are at least twice those determined previously, but these values were obtained at considerably lower ionic strength (Foxall et al., 1979; Thompson and Pownall, 1989; Cicerone et al., 1992). For the 0.05M NaCl electrolyte (the lowest concentration investigated), the predicted diffuse layer thickness at the ionic strength corresponding to the IEP (0.8M) is very small (the Debye length is 0.342nm). Given that the calcium ion has a hydrated diameter of 0.59nm (Diebler et al, 1969), it is not clear whether such a diffuse layer thickness is physically meaningful as it cannot accommodate even a single calcium ion. Vinogradov et al. (2010) suggested that the diffuse layer thickness decreases until it reaches the radius of the hydrated counter-ion, and then remains constant regardless of increasing ionic strength. However, their model does not account for changes in the Stern layer capacitance with changing ionic strength, and cannot explain the data reported here.

Figure 9b shows the effect of varying SO_4 concentration, comparing our data obtained for the 0.5M NaCl electrolyte against that of Zhang and Austad (2006). These are the only comparable data for SO_4 reported previously. Both datasets yield a linear relationship between zeta potential and pSO_4, although the gradient of the linear regression is smaller for the Zhang and Austad data than that obtained here. As discussed in the next section, we suggest this is a consequence of the differing measurement methods: Zhang and Austad used the EPM, in contrast to the SPM used here. Moreover, extrapolating the linear regression in each case to obtain the IEP suggests very different values in terms of pSO_4.

In the single PDI experiments reported here (Figs. 5, 6), precipitation of salts such as $CaSO_4$ and $MgCO_3$ in the pore-space was prevented because each PDI (Ca, Mg or SO_4) was added to NaCl-EQ electrolyte containing only trace or zero concentration of cations or anions other than Na and Cl. Moreover, in the experiments utilising seawater (SW) and formation brine (FMB), we saw no evidence that these salts were deposited. There was no decrease in the concentration of Ca, Mg and SO_4 ions in the equilibrated electrolyte within experimental error, inconsistent with the deposition of salts containing these ions. Indeed, when adding SO_4 we observed a small increase in Ca concentration during equilibration. We also observed no decrease in permeability, or increase in sample mass, within experimental error, and no solids were observed in the effluent electrolyte. Moreover, we note that the zeta potential obtained using FMB was the same within experimental error as the zeta potential obtained by adding a comparable amount of Ca to 2M NaCl electrolyte, suggesting the presence of Ca, Mg and SO_4 did not cause any compositional change at the mineral surfaces.

Effect of electrokinetic measuring technique

A common difference between our data and that reported in previous studies is that we use the SPM to obtain the zeta potential, whereas previous studies have primarily used the EPM. Several studies have suggested that the two methods may yield different results (e.g. Vernhet et al, 1994; Delgado et al., 2007). To test this, we compare zeta potential measurements obtained using both methods on the Portland Limestone, varying pCa in 0.05M NaCl electrolyte (Figure 10). We find that the IEP is identical within experimental error, although uncertainty in the IEP derived from the EPM data is significantly greater than for the SPM data, because positive and negative values of zeta potential were observed across a range of pCa (0.71-0.50). There was no such ambiguity in the SPM data.

Both methods also yield a linear relationship between zeta potential and pCa, although the gradient of the linear regression obtained from the EPM data is twice that obtained from the SPM data (-10.45±0.55 mV/decade for the EPM versus -5.10 ± 0.47 mV/decade for the SPM). We fit the EPM data using equation 5 and the values reported in Table 3, assuming $\Delta = 0$ (i.e. assuming the shear plane corresponds with the Stern plane) in common with previous studies using the EPM on calcite (Foxall et al., 1979; Thompson and Pownall, 1989; Pierre et al. 1990; Cicerone et al., 1992). We then fit our SPM data using the same parameters, but adjusting Δ to obtain a match, yielding a value of 0.245nm. This is a very small offset for the shear plane, and reflects the very small thickness of the diffuse layer at the IEP as discussed in the previous section. Nonetheless, the difference in gradient is consistent with that expected when there are differences in the relative position of the shear plane in natural porous media and powder suspensions. The complex geometry of natural pore-spaces, including the presence of sharp-angled corners and crevices, means that the effective location of the shear plane lies further from the mineral surface than in powder suspensions. SPM measurements are more relevant when quantifying the zeta potential of natural samples, because the measurements reflect the mineral surfaces that predominantly interact with the adjacent fluids.

Effect of NaCl concentration on the IEP

No previous studies have determined the IEP for natural and artificial calcite expressed as pMg, but several have reported values of the IEP expressed as pCa (Table 4). The values observed are typically much higher (i.e. the IEP was observed at lower calcium concentration) than those determined here. Only Chen et al. (2014) have observed the IEP at a comparably low value of pCa; they investigated natural limestone consistent with our study, but employed the EPM method and DIW electrolyte, rather than the SPM and NaCl electrolytes used here. It is not

clear why the IEP for natural Portland limestone occurs at such low values of pCa compared to the majority of previous studies. Pierre et al. (1990) suggested that the IEP is governed by the relative magnitude of the equilibrium constants K_{Ca} and K_{CO3} governing the adsorption of Ca and CO_3 ions on the calcite mineral surface. The IEP shifts to lower pCa if $K_{CO3} > K_{Ca}$; that is, if the calcite surfaces show greater affinity for CO_3 than Ca. Pierre et al. (1990) found the IEP differed for synthetic and natural calcite and argued that this reflected the differing affinity for Ca and CO_3.

The Pierre et al. model suggests that the natural Portland limestone investigated here has a much greater affinity for CO_3 than Ca. Thus, the difference may be related to sample type: most previous studies used synthetic calcite or natural chalk, rather than the natural limestone used here. It may also be related to the pH and/or the establishment of the initial equilibrium conditions. Thompson and Pownall (1989) and Cicerone et al. (1992) conducted experiments over the pH range 7-11 and 8.5-10.5 respectively; the higher pH values do not represent equilibrium conditions. Zhang et al. (2006) and Chen et al. (2014) kept the pH fixed at 8.4 and 8 respectively, but do not report the pre-equilibration steps used here. The pH was fixed in our experiments by the procedure used to ensure the sample was in equilibrium with the electrolyte prior to starting the experimental measurements.

We have also found that the IEP for Portland limestone decreases with increasing NaCl concentration over the range 0.05M – 0.5M. Previous studies have argued that the IEP is independent of NaCl concentration, as Na and Cl are indifferent ions to the calcite surface (e.g. Pierre et al., 1990). We suggest that the difference in IEP between the 0.05M and 0.5M/2M NaCl electrolytes observed here is due to the reduced ability of the calcium ions to interact with the calcite surface, owing to (i) the collapse of the double layer and (ii) increasing occupancy of the diffuse part of the double layer by hydrated sodium ions, which have a smaller radius than the calcium ions at 0.47nm (Vinogradov et al., 2010). However, we note this

hypothesis fails to explain the data of Chen et al. (2014), as they observed a comparable IEP to ours at much lower NaCl concentration.

Implications for controlled salinity waterflooding (CSW)

We have shown that the zeta potential of intact natural limestone samples is positive at elevated Ca and Mg concentration below the IEP (pCa = pMg = 0.63 – 0.41 as discussed above) and becomes negative as the Ca and or Mg concentration is decreased; it also becomes increasingly negative as the SO_4 concentration is increased. We have also shown that the zeta potential of natural limestone saturated with formation brine, rich in Ca ions, is positive, consistent with previous studies (Jackson and Vinogradov, 2012; Chen et al., 2014; Mahani et al., 2015; see Figure 9a). In such formations, an attractive electrostatic force will act between the positively charged mineral surfaces and the negatively charged oil-brine interface, promoting wettability alteration to oil-wet conditions (e.g. Buckley et al., 1989). However, if the concentration of Ca or Mg in the injection brine during controlled salinity waterflooding (CSW) is decreased below the IEP, the zeta potential changes polarity to negative leading to electrostatic repulsion, which may lead to wettability alteration to more water-wet conditions, releasing previously adsorbed crude oil from the calcite mineral surfaces and therefore improving oil recovery. It has been shown by Jackson and Vinogradov (2012) that more water-wet conditions in natural carbonate samples correlate with a more positive zeta potential.

Previous reported values of the IEP expressed as pCa suggest that considerable reduction in Ca concentration is required to change the polarity of calcite (Table 4; see also Fig. 9a); however, our results suggest that reducing the concentration of Ca in the injection brine (selectively or by bulk dilution) by a factor of only 2 relative to the formation brine can lead to inversion of the surface charge. Injection of seawater will also cause inversion of the calcite surface charge, because of the lower Ca concentration and higher SO_4 concentration. This can explain why improved recovery in carbonates during CSW has been observed in response to relatively

minor levels of injection brine dilution, compared to sandstones in which improved recovery is only observed for very low salinity injection brines (<0.05M; see Jackson et al., 2015 for a review).

Previous studies have also suggested that improved oil recovery in corefloods or spontaneous imbibition (SI) experiments can be observed by either diluting seawater as the injection fluid (Yousef et al., 2011), or adding SO_4 to seawater as the imbibing fluid (Zhang and Austad, 2006). In one case, the total ionic strength is simply decreased; in the other, the ionic strength is increased but the relative concentration of ions is changed. Here we show the change in zeta potential is almost identical; diluting seawater and adding SO_4 causes the negative zeta potential to increase in magnitude i.e. become more negative (Figure 7). As discussed above, this can cause wettability alteration to more water-wet conditions and release previously trapped oil in coreflooding experiments, or cause increased imbibition in SI experiments. Simple dilution causes expansion of the double layer and hence a more negative zeta potential (Ligthelm et al, 2009; Nasralla and Nasr-El-Din, 2014); addition of SO_4 yields a more negative zeta potential by increasing the negative charge on the calcite mineral surface (e.g. Fig. 5). Figure 11 shows the incremental recovery observed by diluting seawater, or adding SO_4 to seawater, in the experiments reported by Yousef et al. (2011) and Zhang and Austad (2006), plotted against the change in zeta potential we observed here by modifying the composition of seawater in the same way. There is a clear correlation between increasingly negative zeta potential change and improved recovery, irrespective of how the seawater composition is changed. We suggest that a similar change in zeta potential occurred during the experiments of Yousef et al. (2011) and Zhang and Austad (2006), but was unrecorded because the zeta potential was not measured. However, we note that the samples and experimental methods and conditions are inconsistent across the three sets of experimental results correlated in Figure 11. Future work relevant to CSW should focus on testing the link between brine composition, zeta

potential and increased oil recovery using integrated experiments with consistent materials and experimental conditions.

One final point relevant to CSW relates to the repeatability of laboratory coreflooding experiments. In many studies, a small number of samples are used repeatedly and are cleaned in between experiments. The cleaning protocol typically focuses on ensuring that crude oil is removed from the pore-space. However, we show here that standard cleaning protocols does not restore the zeta potential to its pristine state. This may impact on how the surfaces interact with PDIs in the aqueous phase and polar species in the oil phase, during aging and subsequent waterfloods. If the zeta potential is not returned to its pristine state then the experiments may not be repeatable. We recommend the zeta potential is measured on intact samples before, during and after controlled salinity waterflooding experiments to constrain the behaviour of this key surface property.

Conclusions

We report here measurements of the zeta potential on intact Portland limestone obtained primarily using the streaming potential method (SPM), supplemented by a smaller number of measurements of the more widely applied electrophoretic mobility method (EPM). The experiments were designed to determine how the zeta potential is affected by the concentration of Ca, Mg and SO_4 over the range found in natural brines, and also how the zeta potential is affected by the concentration of these potential-determining ions in the presence of Na and Cl over the range found in natural brines. Our approach contrasts with many previous studies because the experimental method is specifically designed to ensure the equilibrium achieved between rock and electrolyte is consistent with natural processes. The results are directly applicable to a wide variety of natural systems including carbonate oil reservoirs and deep saline aquifers. The key findings can be summarized as follows:

- Ca and Mg change the zeta potential of intact natural limestone samples, causing a decrease in magnitude of the negative zeta potential with increasing concentration and causing polarity inversion to positive zeta potential at high concentration. We show for the first time that the two PDIs behave identically within experimental error, and the zeta potential varies linearly with both pCa and pMg over the broad range found in natural brines.
- SO_4 changes the zeta potential of natural limestone, causing an increase in the magnitude of the negative zeta potential with increasing concentration, and the zeta potential varies linearly with pSO_4 over the broad range found in natural brines. However, the gradient of the liner regression is lower than for Ca and Mg.
- We show for the first time that the IEP (expressed as pCa or pMg) decreases with increasing NaCl concentration. We report considerably lower values of IEP than most previous studies of calcite and chalk, and suggest that this may result from differences in the mineral surfaces (synthetic and natural calcite, natural chalk) compared to the natural limestone investigated here, and the careful method used to establish the initial equilibrium conditions between sample and electrolyte. We recommend this method in all studies of natural carbonates.
- We show for the first time that the IEP (expressed as pCa) obtained using SPM and EPM measurements on the same Portland Limestone are identical within experimental error, but the error is much larger for the EPM method. Both methods show a linear relationship between zeta potential and pCa, but the gradient is a factor of two larger for the EPM method, consistent with a change in the location of the shear plane. SPM measurements are more relevant when quantifying the zeta potential of natural porous samples, because the measurements reflect the mineral surfaces that predominantly interact with the adjacent fluids.

- Standard laboratory cleaning protocols do not return carbonate mineral surfaces to a repeatable ‘pristine’ state, which may affect the repeatability of subsequent experiments on the same sample, including the coreflooding/spontaneous imbibition experiments used to investigate controlled salinity waterflooding.
- Changes in wettability and oil recovery during controlled salinity waterflooding are consistent with the changes in zeta potential observed here. Carbonates saturated with formation brine rich in Ca are likely to have positively charged mineral surfaces (electrostatic attraction), encouraging wettability alteration to oil-wet conditions. Injecting seawater or diluted formation brine can reduce the Ca and/or Mg concentration below the IEP; note that the lower IEP observed here suggests that much less dilution is required than predicted previously. This yields negatively-charged mineral surfaces (electrostatic repulsion), increasing recovery by releasing previously trapped oil. Diluting seawater, or adding SO_4, both yield increasingly negative zeta potential, consistent with experimental studies that report improved recovery in both cases.

Acknowledgements

TOTAL are thanked for supporting Jackson under the TOTAL Chairs program at Imperial College, and Vinogradov through the TOTAL Laboratory for Reservoir Physics at Imperial College where the SPM measurements were conducted. Saudi Aramco EXPEC ARC are thanked for providing access to their zetameter which was used to conduct the EPM measurements.

References

Alotaibi MB, Nasr-El-Din HA, Fletcher JJ. "Electrokinetics of limestone and dolomite rock particles" SPE Reserv Eval Eng. Vol 14, pp. 594–603. (2011)

Alotaibi, MB and Yousef, AA, "The impact of dissolved species on the reservoir fluids and rock interactions in carbonates", Society of Petroleum Engineers Conference Paper 177983, presented at the SPE Saudi Arabia Section Annual Technical Conference and Exhibition (2015)

Amankonah, J. O., and Somasundaran, P. "Effects of dissolved mineral species on the electrokinetic behavior of calcite and apatite" Journal of Colloids and Surfaces, Vol. 15, pp. 335-353. (1985)

Appelo, C.A.J. "Cation and proton exchange, pH, variations, and carbonate reactions in a freshening aquifer" Water Resources Research, Vol 30, pp. 2793–2805. (1994)

Bakiewicz, W., Milne, D.M., Noori, M. "Hydrogeology of the Umm Er Radhuma aquifer, Saudi Arabia, with reference to fossil gradients" Q. J. Eng. Geol., Vo. 15, pp. 105–126 (1982)

Buckley, J.S., Takamura, K. and Morrow, N.R., "Influence of Electrical Surface Charges on the Wetting Properties of Crude Oils", SPE Res. Eng. Vol. 4, pp. 332-40. (1989)

Buckley, J.S., Liu, Y. and Monsterleet, S., "Mechanisms of Wetting Alteration by Crude Oils", SPE Journal, Vol. 3, pp. 54-61. (1998)

Chen, L, Zhang, G, Wang, L, Wu, W, Ge, J "Zeta potential of limestone in a large range of salinity" Colloids and Surfaces A: Physicochem. Eng. Aspects, Vol. 450, pp. 1-8. (2014)

Cicerone, DS, Regazzoni, AE, Blesa, MA "Electrokinetic properties of the calcite/water interface in the presence of magnesium and organic matter" Colloids and Surfaces A: Physicochem. Eng. Aspects, Vol. 154, pp. 423–433. (1992)

Delgado, AV, González-Caballero, F, Hunter, RJ, Koopal, LK and Lyklema, J. "Measurement and interpretation of electrokinetic phenomena" Journal of Colloid and Interface Science, Vol. 309, pp.194–224. (2007)

Diebler, H., Eigen, M., Ilgenfritz, G. Maas, G., Winkler, R. "Kinetics and mechanism of reactions of main group metal ions with biological carriers" Pure Appl. Chem. Vol. 20, pp. 93–115. (1969)

Eriksson, R, Merta, J and Rosenholm, JB. "The calcite/water interface I. Surface charge in indifferent electrolyte media and the influence of low-molecular-weight polyacrylate" J. of Colloid and Interface Science. Vol. 313, pp. 184-193. (2007)

Foxall, T, Peterson, GC, Rendall, HM, Smith, AL "Charge determination at the calcium salt/aqueous solution interface" J. Chem. Soc. Faraday Trans. Vol. 75, pp. 1034-1039. (1979)

Fuerstenau, M. C., Gutirrrez, G., and Elgillani, D. A. "The influence of sodium silicate in non-metallic floatation systems" Trans. AIME 241, pp. 319-323. (1968)

Garrels, R and Christ C “Solutions, Minerals, and Equilibria” Jones and Bartlett Publishers International, London, pp. 450. (1990)

Gomari, KAR, Hamouda, AA, Denoyel, R “Influence of sulfate ions on the interaction between fatty acids and calcite surface” Colloids and Surfaces A: Physicochem. Eng. Aspects, Vol. 287. (2006)

Gulamali M.Y., Leinov E., and Jackson M. D. “Self-potential anomalies induced by water injection into hydrocarbon reservoirs” Geophysics, Vol. 76, pp. 283–292. (2011)

Heberling, F, Trainor, TP, Lutzenkirchen, J, Eng, P, Denecke, MA, Bosbach, D "Structure and reactivity of the calcite-water interface" Journal of Colloid and Interface Science. Vol. 354, pp. 843–857. (2011)

Huang, YC, Fowkes, FM, Lloyd, TB, Sanders, ND “Adsorption of calcium ions from calcium chloride solutions onto calcium carbonate particles” Langmuir, Vol. 7, pp. 1742-1748. (1991)

Hunter, R. J. “Zeta Potential in Colloid Science” Academic Press, New York. (1981)

Hunter, R. J. “Recent developments in the electroacoustic characterisation of colloidal suspensions and emulsions” Colloids and Surfaces A: Physicochem. Eng. Aspects. Vol. 141, pp. 37-66. (1998)

Jackson, M.D. and Vinogradov, J. “Impact of wettability on laboratory measurements of streaming potential in carbonates” Colloids and Surfaces A: Physiochem. Eng. Aspects. Vol. 393, pp. 86-95. (2012a)

Jackson, M.D., Gulamali M.Y., Leinov E., Saunders, J. H., Vinogradov, J. “Spontaneous Potentials in Hydrocarbon Reservoir during Waterflooding: Application to Water-Front Monitoring” Society of Petroleum Engineers Journal. Vol. 17, pp. 53-69. (2012a)

Jackson, M.D., Butler, A.P., Vinogradov, J. “Measurements of spontaneous potential in chalk with application to aquifer characterization in the southern UK” Quarterly Journal of Engineering Geology and Hydrogeology, vol. 45, pp. 457 –471. (2012b)

Jackson, M.D. “Self-potential: Tools and techniques” in: Treatise on Geophysics (editor in chief: G. Schubert), 2nd edition, volume 11, chapter 9, Elsevier. (2015)

Jouniaux, L., and J. P. Pozzi “Streaming potential and permeability of saturated sandstones under triaxial stress: consequences for electro-telluric anomalies prior to earthquakes” J. Geophys. Res., Vol.100 (B6), pp. 10,197‑10,209. (1995)

Kasha, A, Al-Hashim, H, Abdallah, W, Taherian, R, Saurerer, B “Effect of Ca, Mg and SO4 ions on the zeta potential of calcite and dolomite particles aged with stearic acid” Colloids and Surfaces A: Physicochem. Eng. Aspects, Vol. 482, pp. 290-299. (2015)

Krauskopf, Konrad B. “Introduction to Geochemistry” 2nd Edition. McGraw-Hill International, New York. (1982)

Ligthelm, D.J.,Gronsveld, J., Hofman, J.P. ”Novel waterflooding strategy by manipulation of injection brine composition” EUROPEC/EAGE Conference and Exhibition, Amsterdam. SPE119835 (2009)

Madsen, L “Surface Charge of Calcite” Encyclopedia of Surface and Colloid Science, Marcel Dekker Inc., New York, Vol. 4, pp. 3978-3992. (2002)

Mahani, H, Keya, AL, Berg, S, Bartels, WB, Nasralla, R, and Rossen, WR “Insights into the Mechanism of Wettability Alteration by Low-Salinity Flooding (LSF) in Carbonates” Energy Fuels, Vol. 29, pp. 1352–1367. (2015a)

Mahani, H, Keya, AL, Berg, S, Bartels, WB, Nasralla, R, and Rossen, WR “Driving mechanisms of low salinity waterflooding in carbonate rocks, SPE paper 174300 (2015b).

Meece, DE, Benninger, LK “The coprecipitation of Pu and other radionuclides with $CaCO_3$” Geochim. Cosmochim. Acta, Vol 57, pp. 1447-1458. (1993)

Mishra, SK “The electrokinetics of apatite and calcite in inorganic electrolyte environment” International Journal of Mineral Processing, Vol. 5, pp. 69-83. (1978)

Morse, JW. “The Surface Chemistry of Calcium Carbonate Minerals in Natural Waters: An Overview” Marine Chemistry, 20, pp. 91-112. (1986)

Morse, JW and Mackenzie, FT “Geochemistry of sedimentary carbonates” Elsevier, Amsterdam. (1990)

Nasralla RA, Nasr-El-Din HA. “Double-layer expansion: is it a primary mechanism of improved oil recovery by low-salinity waterflooding?” SPE Reserv Eval Eng. Vol. 17, pp. 49–59. (2014)

Pierre, A, Lamarche, JM, Mercier,RFoissy, A and Persello, J. “Calcium As Potential Determining Ion in Aqueous Calcite Suspensions” J. of Dispersion Science and Technology, Vol.11: pp. 611-635. (1990)

Plummer, L. N. and Busenberg, G. E. “ The solubilities of calcite, aragonite and vaterite in CO2 H2O solutions between 0 and 90 C and an evaluation of the aqueous model for the system CaCO3-CO2–H2O.” Geochim. Cosmochim. Acta. Vol. 46, pp. 1011–1040. (1982)

Pokrovsky, O.S., Golubev, S.V., Schott, J.“Dissolution kinetics of calcite, dolomite and magnesite at 25 C and 0 to 50 atm pCO2.” Chemical Geology. Vol 217, pp. 239–255. (2005)

Reeder, RJ Nugent, M Tait, CD Morris, DE Heald, SM Beck, KM Hess, WP and Lanzirotti, A “Coprecipitation of Uranium(VI) with Calcite: XAFS, micro-XAS, and luminescence characterization” Geochim. Cosmochim. Acta. Vol. 65, pp. 3491–350. (2001)

Riley, Nick. “Geological storage of carbon dioxide.” In: Hester, R.E.; Harrison, R.M., (eds.) Carbon capture: sequestration and storage. Cambridge, UK, Royal Society of Chemistry, 155-178. (2010) (Issues in environmental science and technology, 29).

Robins, N.S., Jones, H.K., Ellis, J. “An aquifer management case study: the Chalk of the English South Downs” Water Resources Management, Vol. 13, pp. 205-218. (1999)

Romanuka, J., Hofman, J.P., Ligthelm, D.J., Suijkerbuijk, B.M.J.M. Marcelis, A.H.M., Oedai, S., Brussee, N.J., van der Linde, H.A., Aksulu, H., Austad, T “Low Salinity EOR in Carbonates" SPE Improved Oil Recovery Symposium, 14-18 April 2012, Tulsa, Oklahoma, USA. (2012)

Rosenbauer JR, Koksalan T, Palandri JL. “Experimental investigation of CO2–brine–rock interactions at elevated temperature and pressure: Implications for CO2 sequestration in deep-saline aquifers.” Fuel Process Tech. Vol. 86, pp.1581–97. (2005)

Saunders, J. H., M. D. Jackson, and C. C. Pain “Fluid flow monitoring in oil fields using downhole measurements of electrokinetic potential” Geophysics, 73(5). (2008)

Somasundaran, P and Agar, GE. “The Zero Point of Charge of Calcite” J. Colloid Interface Science Vol. 24: pp. 433-440. (1967)

Sondi, I., Biscan, J., Vdovic, N., Skapin, S. D. “The electrokinetic properties of carbonates in aqueous media revisited” Colloids and Surfaces A: Physicochem. Eng. Aspects, Vol. 342, pp. 84-91. (2009)

Strand, S, Høgnesen, EJ, Austad, T. “Wettability alteration of carbonates-Effects of potential determining ions (Ca and SO_4) and temperature” Colloids and Surfaces A: Physicochem. Eng. Aspects Vol. 275, pp. 1–10. (2006)

Stumm, W. and Morgan, J. “Aquatic Chemistry, Chemical Equilibria and Rates in Natural Waters” 3rd edition, John Wiley & Sons, New York, pp. 1022. (1996)

Thompson, DW and Pownall, PG. “Surface Electrical Properties of Calcite” J. of Colloid and Interface Science, Vol. 131, No. I, pp. 74-82. (1989)

Vdovic, N. “Electrokinetic behaviour of calcite - the relationship with other calcite properties” Chemical Geology, 177, 241–248 (2001)

Vernhet, A, Bellon-Fontaine, MN, Doren, A “Comparison of Three Electrokinetic Methods to Determine the Zeta Potential of Solid Surfaces” J. Chim. Phys. Vol. 91, pp. 1728-1747. (1994)

Vinogradov, J, Jaafar, MZ, Jackson, MD “Measurement of streaming potential coupling coefficient in sandstones saturated with natural and artificial brines at high salinity” J. Geophysical Research, Vol. 115, B12204. (2010)

Vinogradov, J and Jackson, MD “Multiphase streaming potential in sandstones saturated with gas/brine and oil/brine during drainage and imbibition” Geophys. Res. Lett. 38 (2011)

Vinogradov, J. and Jackson, M.D. “The effect of brine composition, concentration, temperature and rock texture on zeta potential and streaming potential coupling coefficient measured in sandstones and sandpack” presented at the Annual Meeting of the American Geophysical Society. (2014)

Yousef AA, Al-Saleh S, Al-Kaabi A, Al-Jawfi MS. “Laboratory investigation of the impact of injection-water salinity and ionic content on oil recovery from carbonate reservoirs” SPE Reserv Eval Eng. Vol. 14, pp. 578–93. (2011)

Yousef, AA, Al-Saleh, S and Al-Jawfi, MS. “Improved/Enhanced Oil Recovery from Carbonate Reservoirs by Tuning Injection Water Salinity and Ionic Content” SPE 154076 (2012)

Zhang, P and Austad, T “Wettability and oil recovery from carbonates: Effects of temperature and potential determining ions.” Colloids and Surfaces A: Physicochem. Eng. Aspects, Vol. 279. (2006)

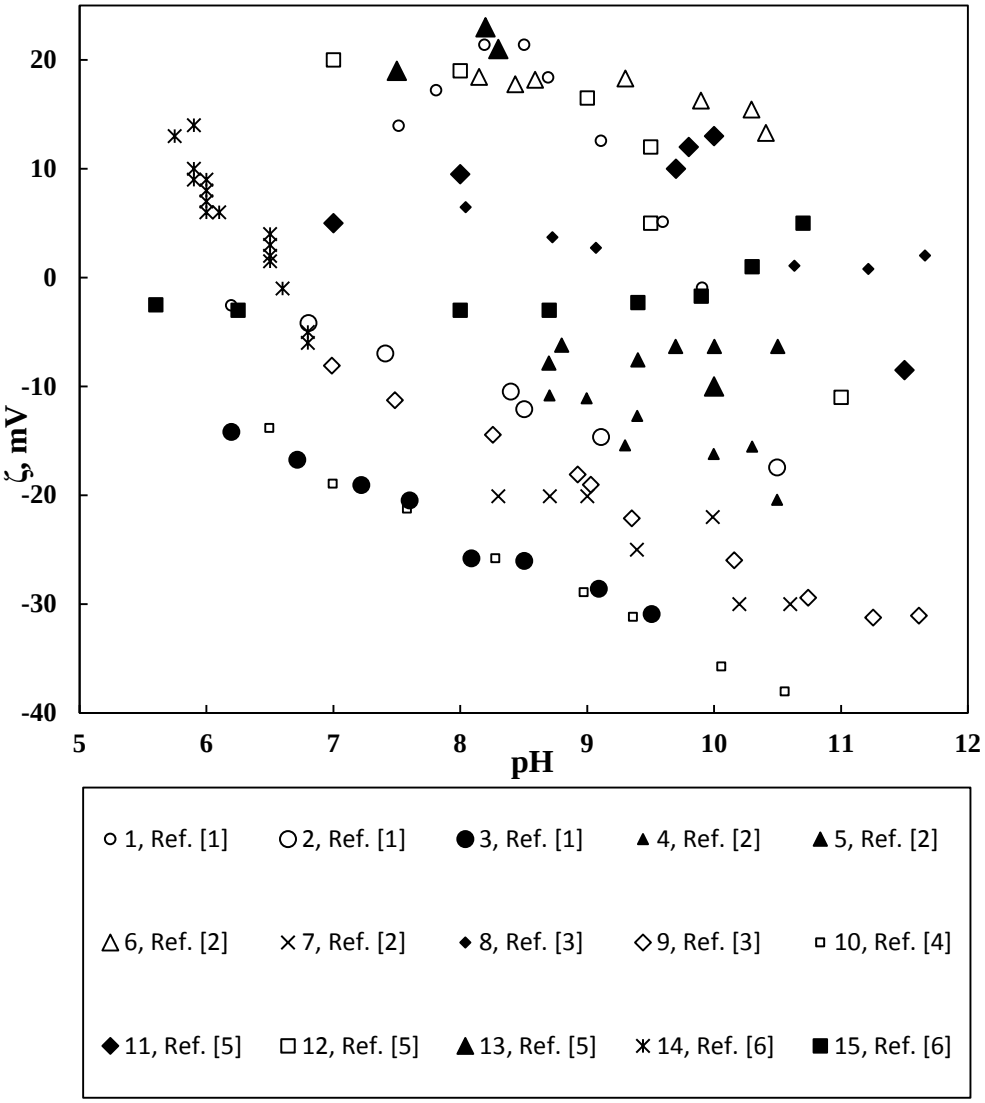

Figure 1. Zeta potential as a function of pH reported on various artificial and natural calcite and limestone samples for various electrolyte compositions and ionic strength. Unless otherwise stated, measurements were obtained using the electrophoretic mobility method (EPM). Vdovic (2001) (Ref. 1) used synthetic calcite (labelled 1), natural limestone (2), and lake sediments (3) in 10^{-3}M NaCl electrolyte. Cicerone et al. (1992) (Ref. 2) used synthetic calcite in 0.03M KCl (4), 0.001M $CaCl_2$ (5) and 0.01M $CaCl_2$ (6) electrolytes, and natural calcite in 0.03M KCl electrolyte (7). Thompson and Pownall (1989) (Ref. 3) used the streaming potential method (SPM) on synthetic calcite in $5x10^{-4}$M $CaCl_2$ (8) and 0.005M NaCl (9) electrolytes. They did not correct for surface electrical conductivity. Sondi et al. (2009)

(Ref. 4) used natural calcite in 0.001M NaCl electrolyte (10). Somasundaran and Agar (1967) (Ref. 5) used the SPM on calcite in deionized water after no mixing (11), mixing for one week (12), and mixing for two months (13). They did not correct for surface electrical conductivity. Heberling et al. (2011) (Ref. 6) used the SPM on calcite in non-equilibrated 0.01M NaCl and 0.005M $CaCl_2$ electrolytes (14), and the EPM on calcite in 0.1M NaCl in equilibrium with $p(CO_2)$=1 bar (15). They did not correct for surface electrical conductivity.

(a)

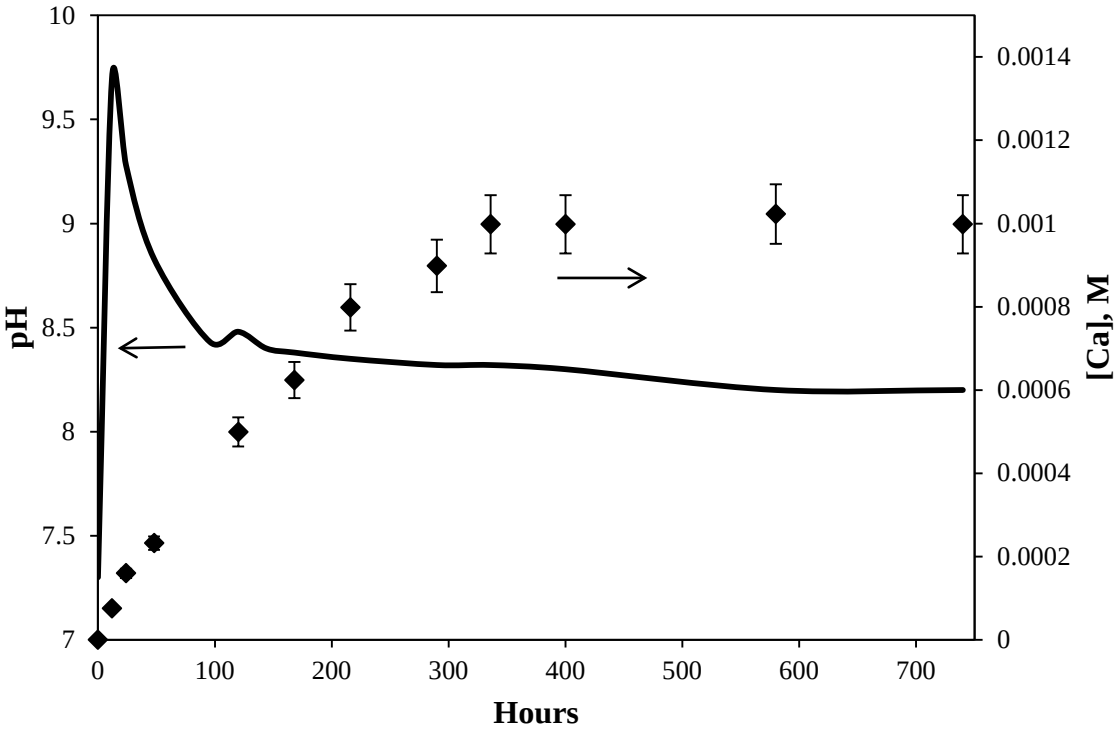

(b)

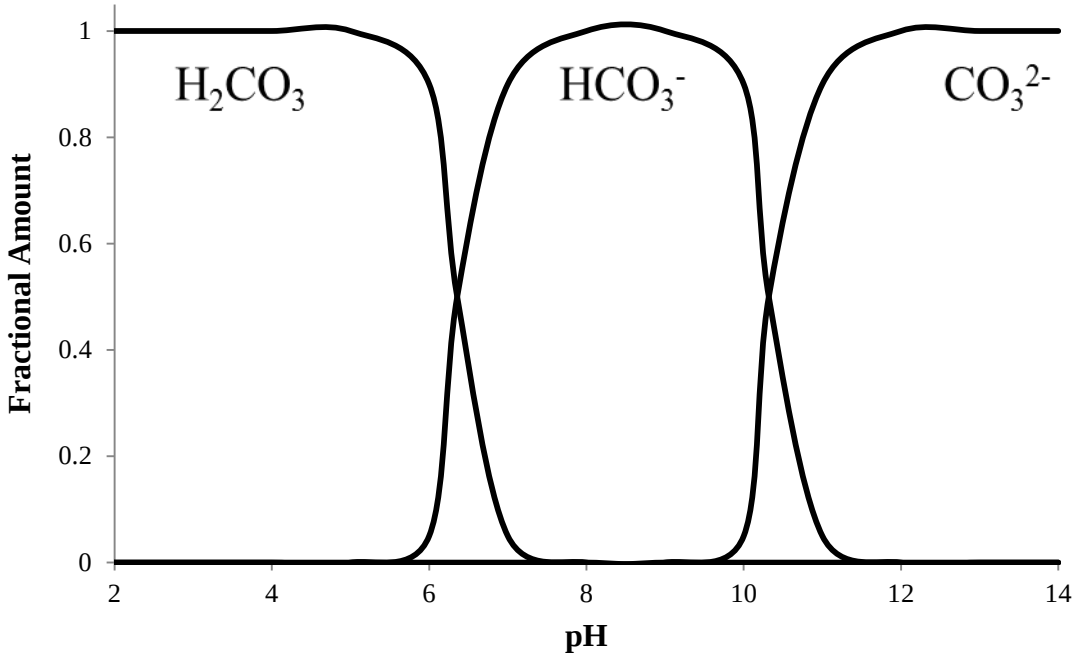

Figure 2. Calcite-water-CO_2 equilibrium for I = 0.05 M NaCl. (a) Calcium concentration and pH measured here as a function of time during equilibration of the natural Portland rock samples with DIW. (b) Carbon speciation into H_2CO_3, HCO_3^-, and CO_3^{2-} as a function of pH (modified after Stumm and Morgan, 1996).

Table 1. Properties of Portland rock samples used in this study.

Sample	Porosity (%)	Permeability (mD)	Formation Factor (F)
P1	20	3	21.3
P2	19.5	2.2	22.4
P3	21	3.5	20.6

Table 2. Composition of the synthetic Formation Brine (FMB) and natural seawater (SW) and derived compositions used in this study. The seawater was twice (½SW), ten times (1/10SW), and twenty times (1/20SW) diluted, and also had SO_4 added to yield twice (2SW), three times (3SW), and four times (4SW) the natural concentration.

Concentration (M)	**FMB**	**SW**	**1/2SW**	**1/10SW**	**1/20SW**	**2SW**	**3SW**	**4SW**
Na	2	0.5	0.25	0.05	0.025	0.5	0.5	0.5
Ca	0.42	0.012	0.006	0.0012	0.0006	0.012	0.012	0.012
Mg	0.07	0.05	0.025	0.007	0.00025	0.05	0.05	0.05
SO_4	0.0033	0.033	0.016	0.0033	0.0016	0.066	0.099	0.13
pH	7.15	8	8	8	8	8	8	8
Total	2.49	0.615	0.107	0.061	0.0107	0.648	0.681	0.715

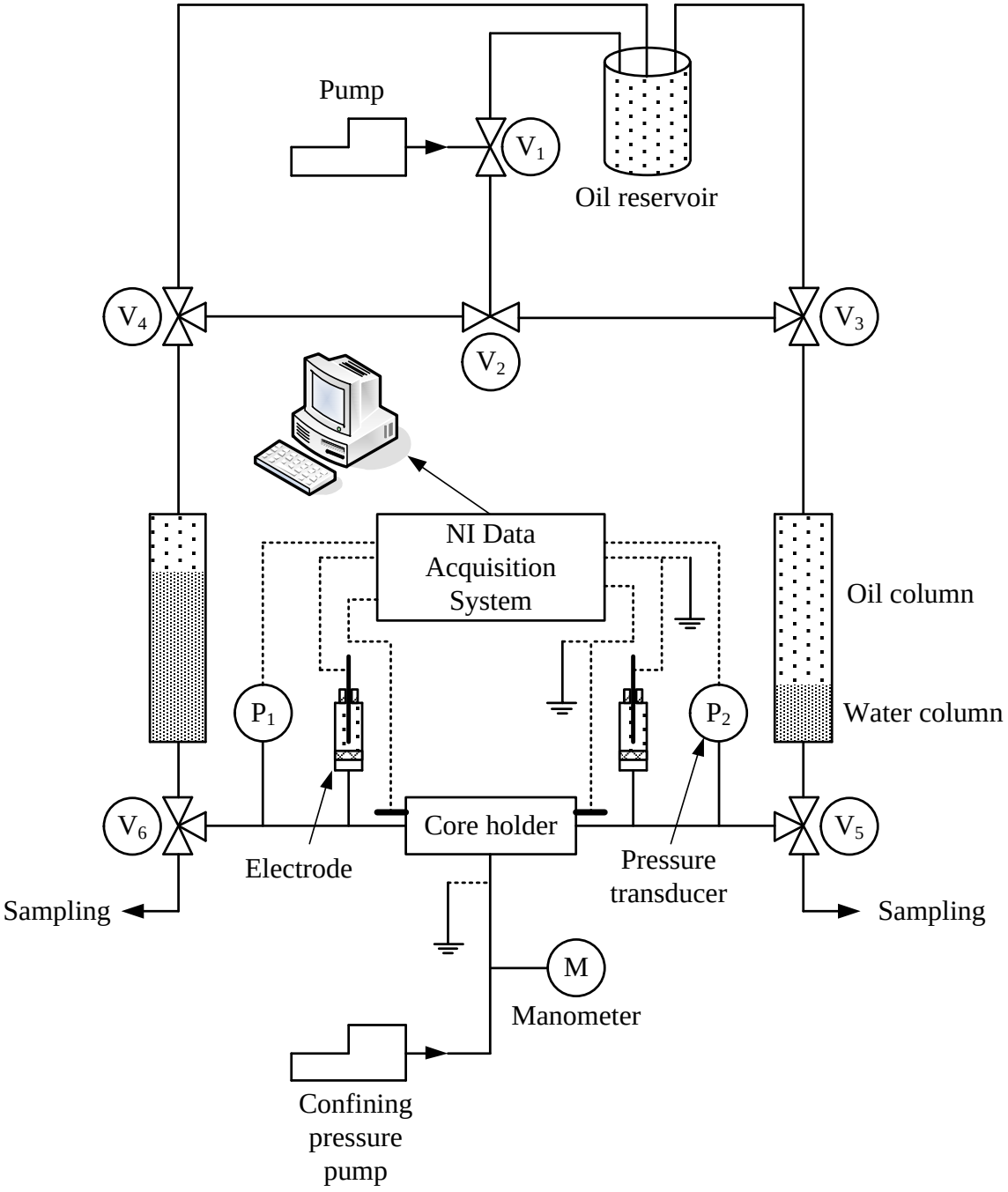

Figure 3. Experimental setup for measuring the streaming potential, which consists of a pressure vessel (core holder), electrolyte reservoirs, pump, flow lines (solid lines) and electrical connections (dashed lines). The oil column in the electrolyte reservoirs serves to isolate the electrolyte from the atmosphere (closed-system). The flow valves $V_1 – V_6$ allow the pump the flow electrolyte through the sample in opposing directions. Modified from Jaafar et al. (2009).

(a)

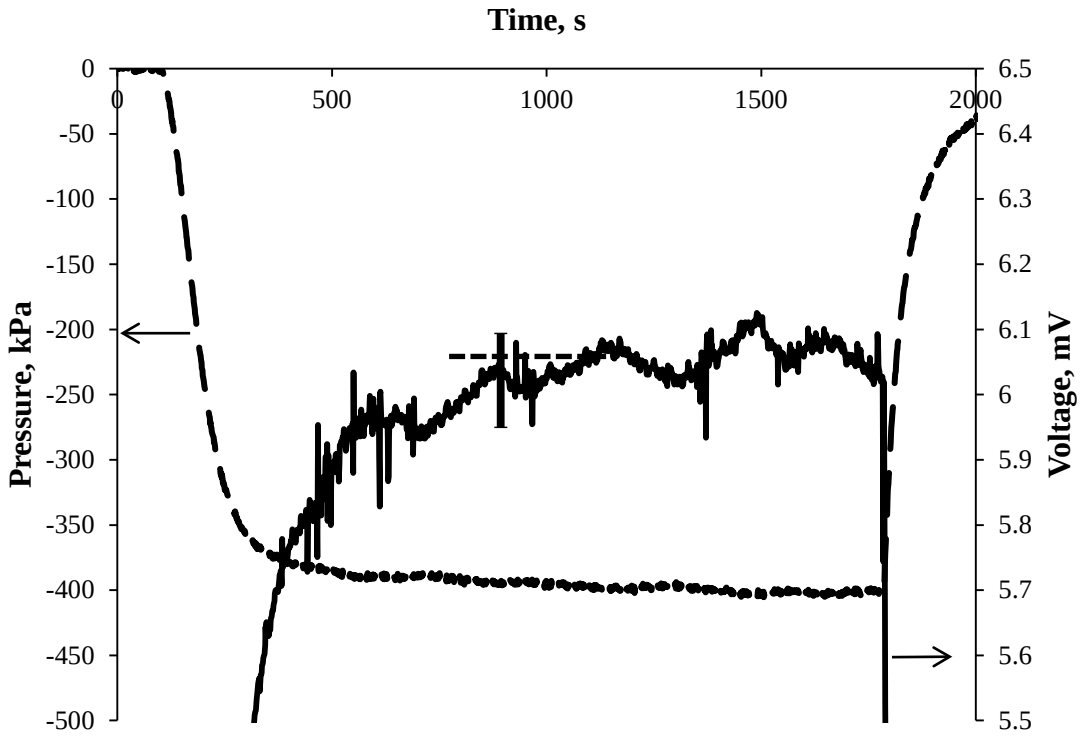
Time, s
Pressure, kPa
Voltage, mV
0
-50
-100
-150
-200
-250
-300
-350
-400
-450
-500
0
500
1000
1500
2000
6.5
6.4
6.3
6.2
6.1
6
5.9
5.8
5.7
5.6
5.5

(b)

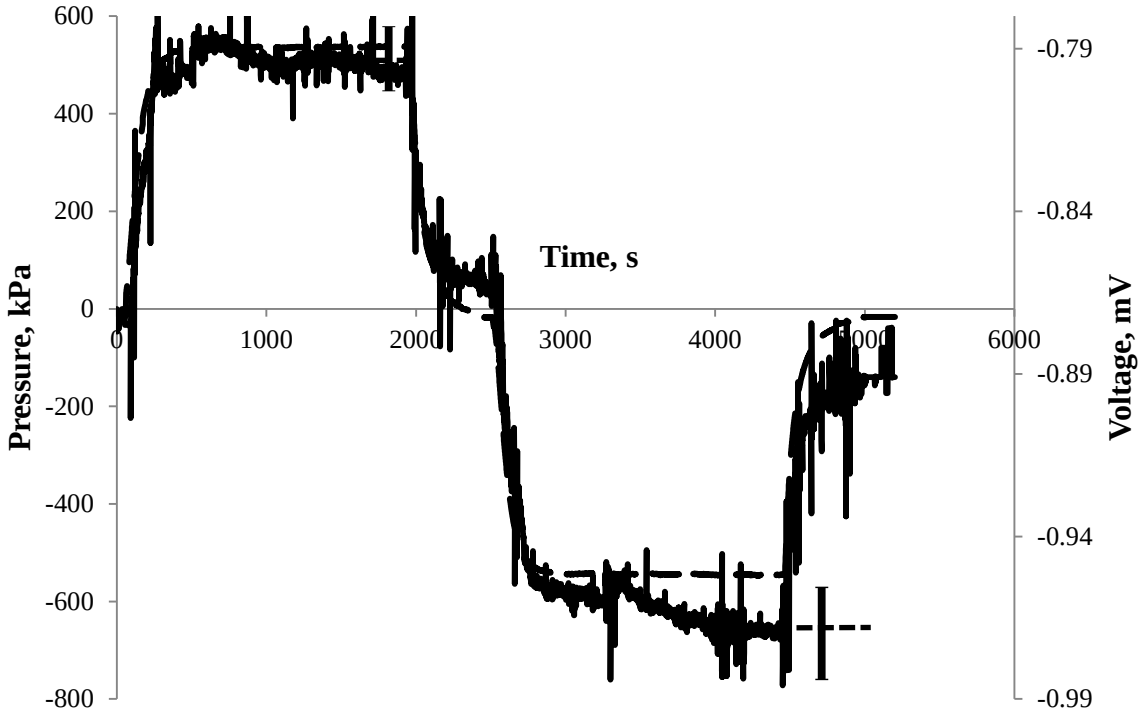
Time, s
Pressure, kPa
Voltage, mV
600
400
200
0
-200
-400
-600
-800
0
1000
2000
3000
4000
5000
6000
-0.79
-0.84
-0.89
-0.94
-0.99

(c)

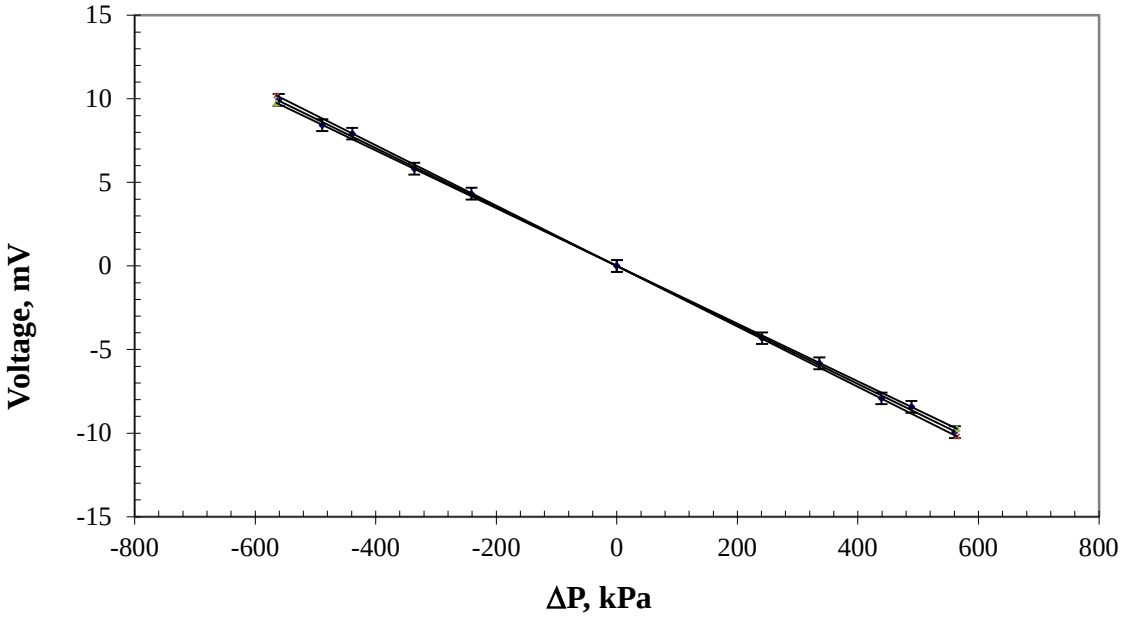

(d)

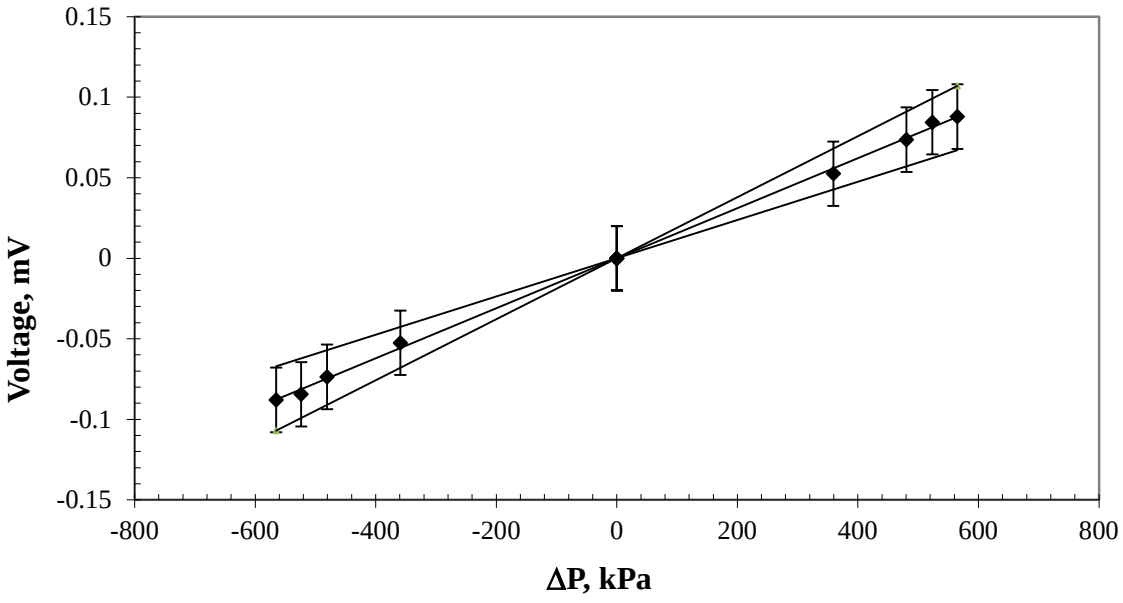

Figure 4. Typical experimental results used to determine the streaming potential coupling coefficient. Plots (a) and (b) show the voltage and pressure variation in experiments at a given flowrate using (a) low ionic strength 0.05M NaCl-EQ electrolyte and (b) high ionic strength synthetic formation brine (FMB). The horizontal dashed lines show the stabilized voltage and

pressure, and the error bar denotes the spread in these values. Plots (c) and (d) show the stabilized voltage plotted against stabilized pressure for the same electrolytes shown in (a) and (b). The gradient of a linear regression through these data yields the streaming potential coupling coefficient.

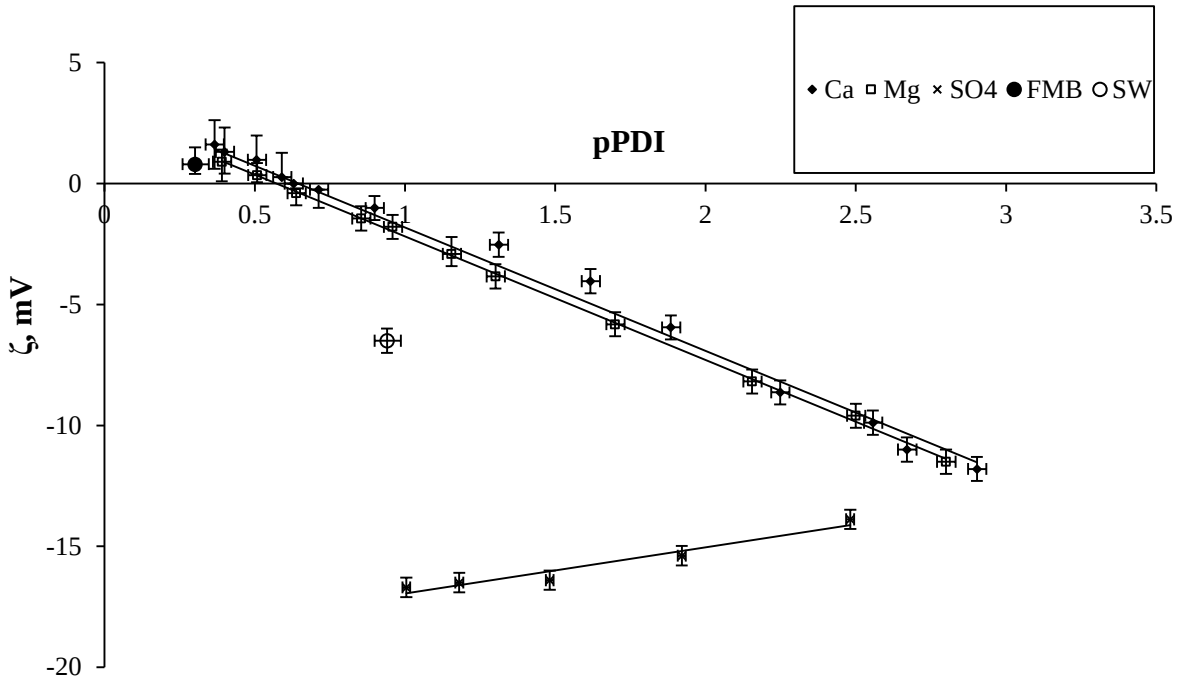

Figure 5. Effect of Ca, Mg and SO_4 concentration (expressed as pPDI) in 0.05M NaCl electrolyte on the zeta potential of Portland limestone. The pH varied in the range 7.2-8±0.3 for the Ca and Mg effluent electrolytes, and 7.9-8±0.3 for the SO_4 effluent electrolytes. Also shown are the results for the synthetic formation brine (FMB) and natural seawater (SW) plotted as a function of pCa + pMg.

(a)

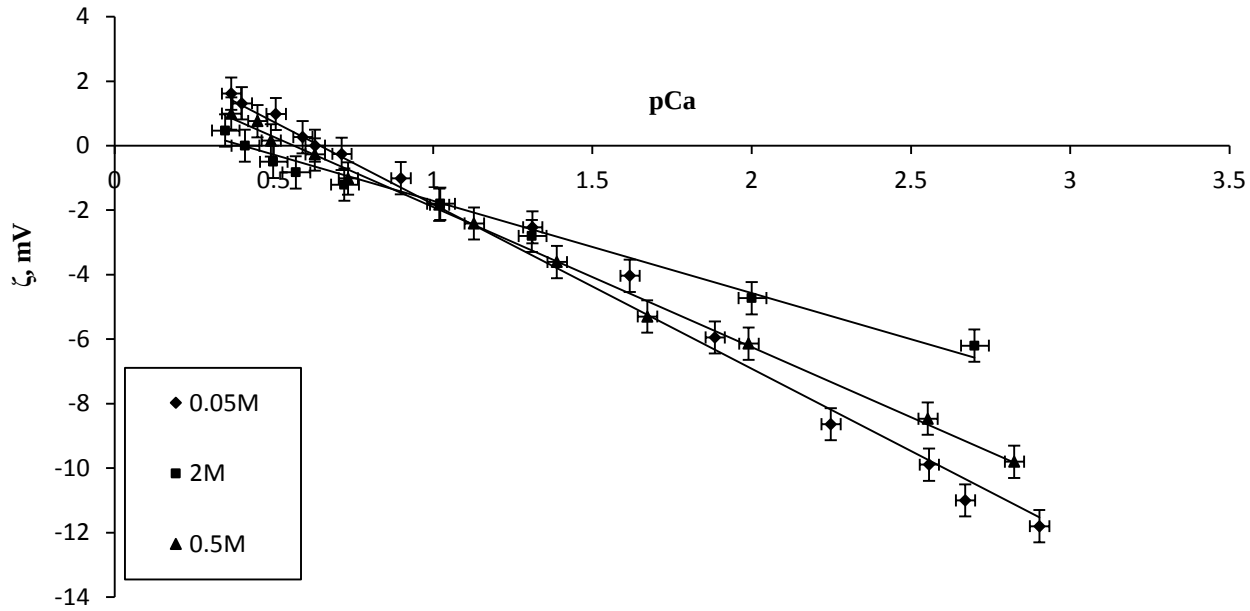
pCa
ζ, mV
4
2
0
-2
-4
-6
-8
-10
-12
-14
0
0.5
1
1.5
2
2.5
3
3.5
0.05M
2M
0.5M

(b)

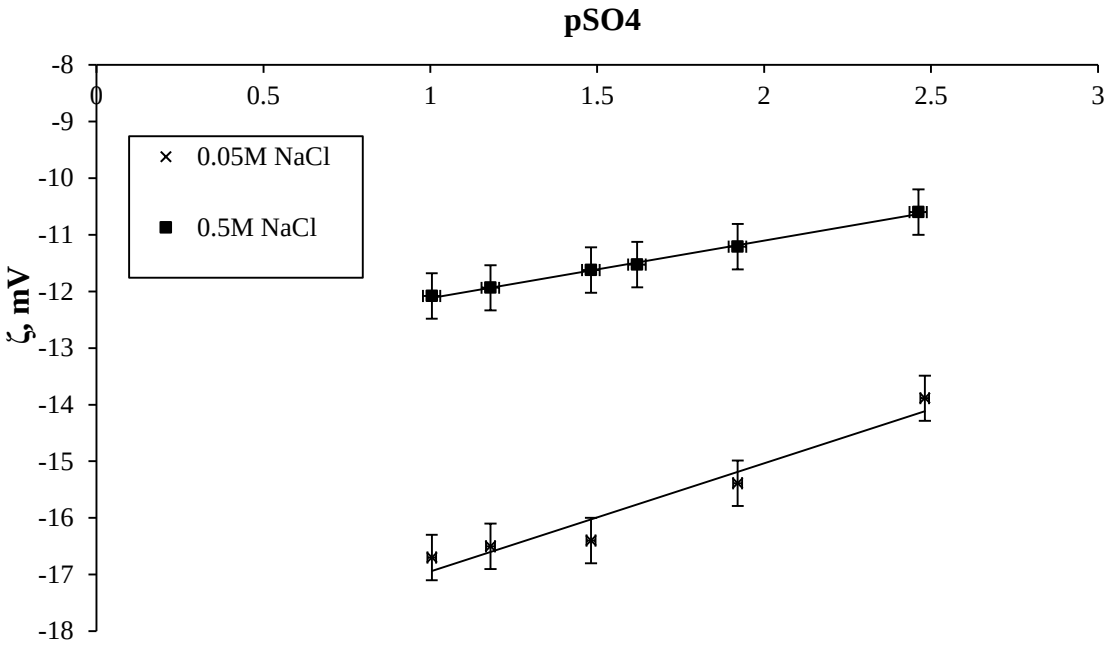
pSO4
ζ, mV
-8
-9
-10
-11
-12
-13
-14
-15
-16
-17
-18
0
0.5
1
1.5
2
2.5
3
0.05M NaCl
0.5M NaCl

(c)

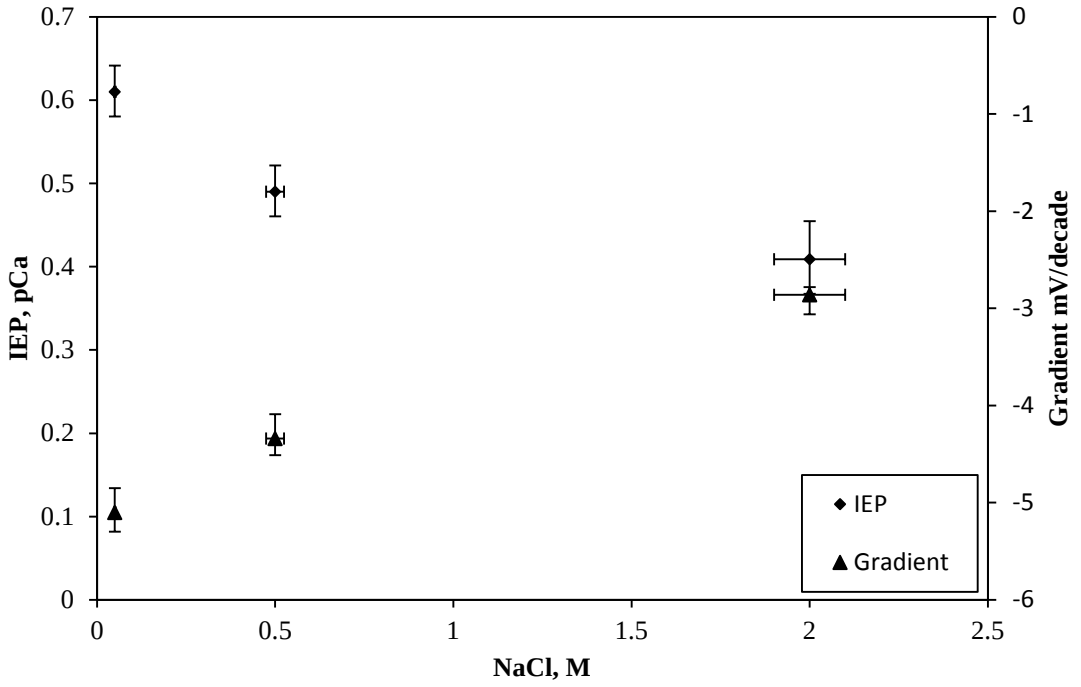

Figure 6. Effect of NaCl concentration on the relationship between PDI concentration and zeta potential of Portland limestone. (a) Effect of Ca concentration (expressed as pCa) in three different NaCl electrolytes (0.05M, 0.5M and 2M) on the zeta potential of Portland limestone, pH in the range 7.2-8±0.3. (b) Effect of SO_4 concentration (expressed as pSO_4) in two different NaCl electrolytes (0.05M, 0.5M) on the zeta potential of Portland limestone, pH in the range 7.9-8.1±0.3. (c) Effect of NaCl concentration on the IEP (expressed as pCa) and zeta potential sensitivity to pCa (expressed as the gradient of the linear regressions shown in (a)).

(a)

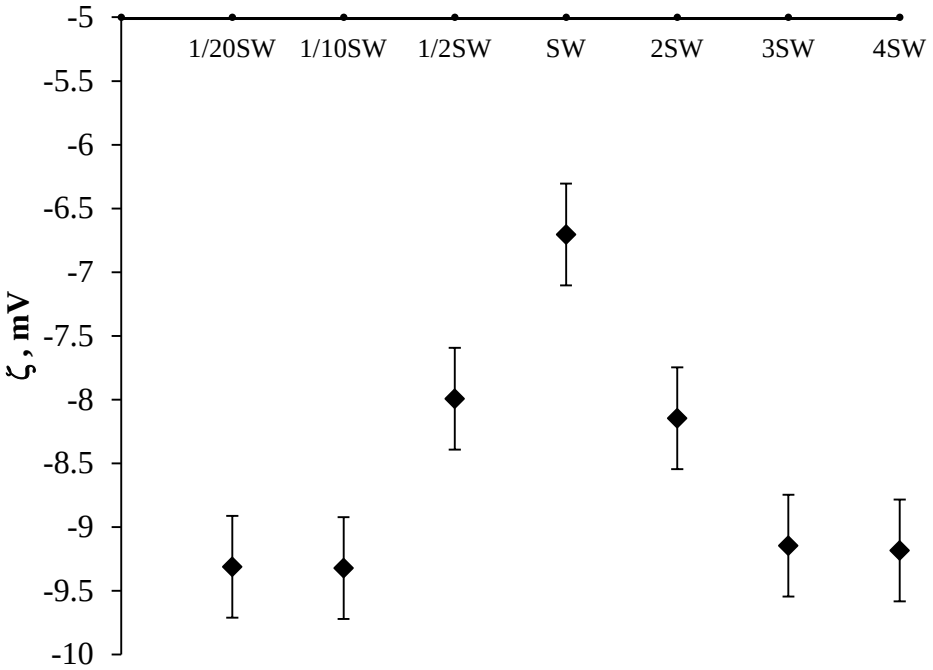

(b)

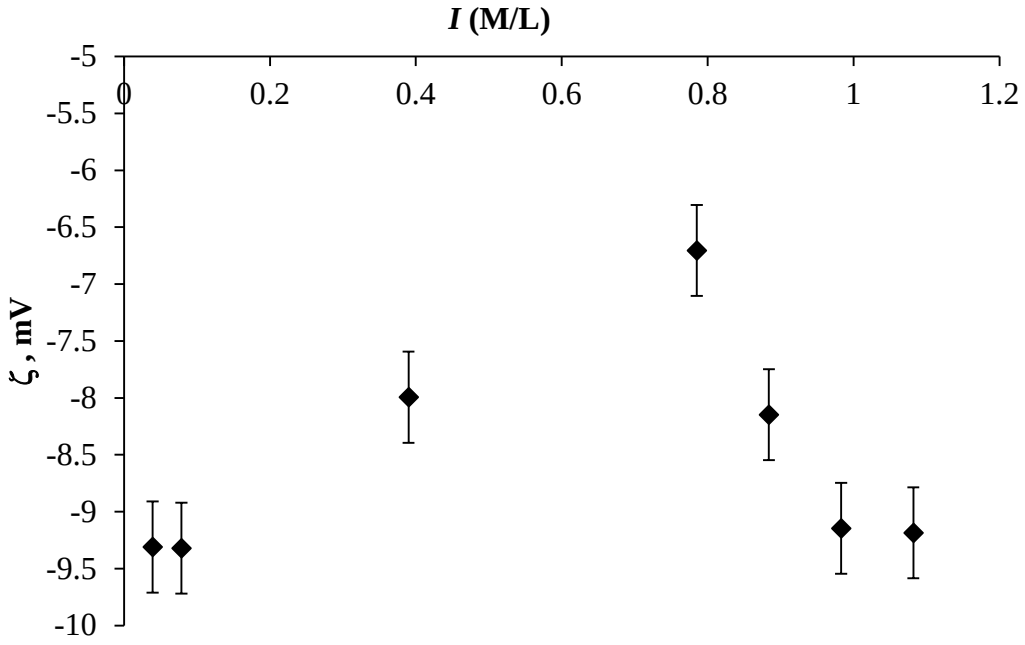

Figure 7. (a) Relationship between zeta potential and electrolyte compositions derived from seawater (SW), pH=8±0.3. (b) Zeta potential of the same compositions plotted as a function of ionic strength (*I*).

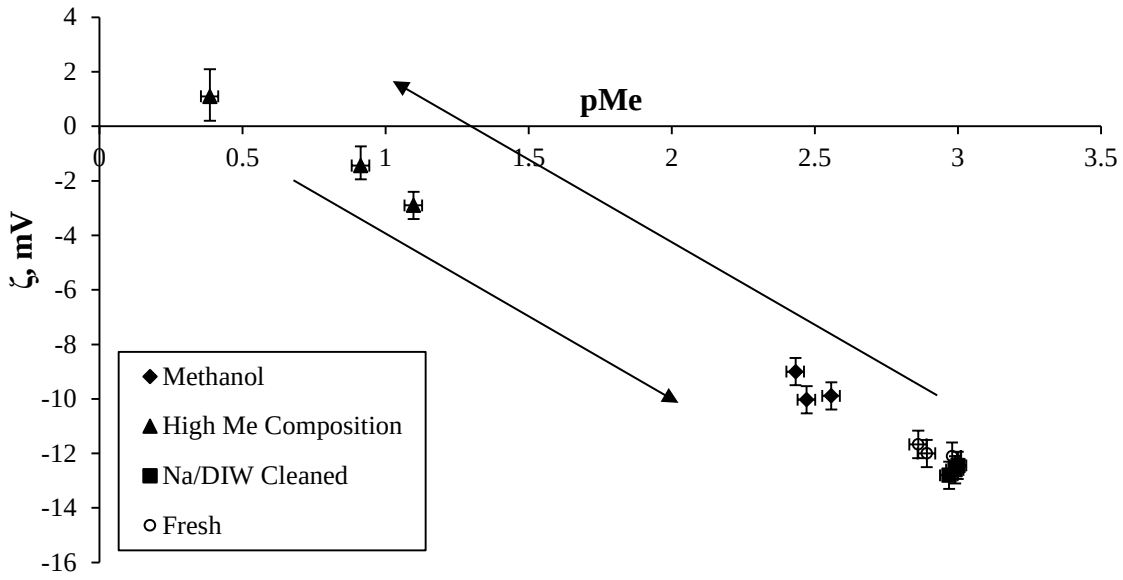

Figure 8. Zeta potential as a function of Ca + Mg concentration (expressed as pMe) for fresh samples (circles), pH = 8.2±0.2, experiments at elevated Ca and Mg concentration (triangles), pH in the range 7.2-7.5±0.3, after standard cleaning with methanol (diamonds), and after the enhanced cleaning with DIW used in this study (squares), pH = 8.2±0.2.

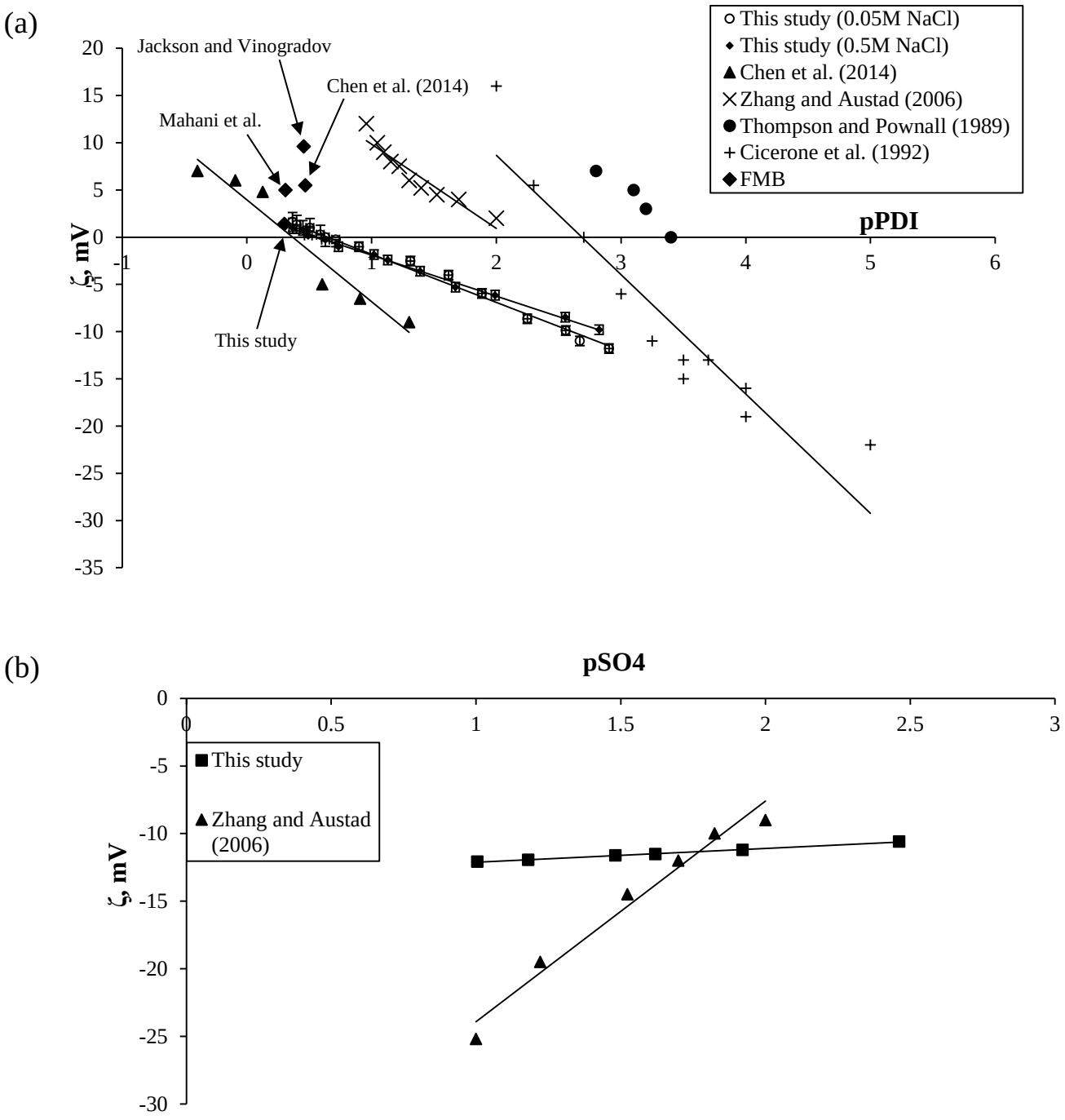

Figure 9. Comparison of the data obtained here and previously published measurements for the zeta potential sensitivity to (a) Ca and (b) SO_4. Errors are shown where reported by the authors. Thompson and Pownall (1989) used the SPM method, synthetic calcite and 0.002M NaCl electrolyte over the pH range 7-11. All other published studies used the EPM method. Cicerone et al. (1992) used synthetic calcite and 0.03M KCl electrolyte over the pH range 8.5-10.5 (error not reported). Zhang et al. (2006) used powered Stevns Klint chalk and 0.573M NaCl electrolyte at pH = 8.4 (error not reported). These

conditions are the most similar to those used here. Chen et al. (2014) used powdered natural limestone and DIW at pH = 8 (error not reported). The various labelled diamonds in (a) show data obtained using natural or synthetic formation brine (FMB).

Table 3. Values of the Stern layer capacitance and shear plane location used to match the experimental data using equation (5). The value of C_s was identified first for the EPM data using $\Delta = 0$, consistent with previous studies. The value of C_s was then fixed for the SPM data at the same NaCl concentration matched by adjusting Δ to account for the complex pore-space. It was not possible to match the other NaCl concentrations tested without further adjusting C_s. The shear plane location is not expected to be significantly affected by the increase in ionic strength.

Method	NaCl concentration (M)	Stern Layer capacitance C_s (F/m^2)	Shear plane location Δ (nm)
EPM	0.05	1.13	0
SPM	0.05	1.13	0.245
SPM	0.5	1.76	0.245
SPM	2	2.75	0.245

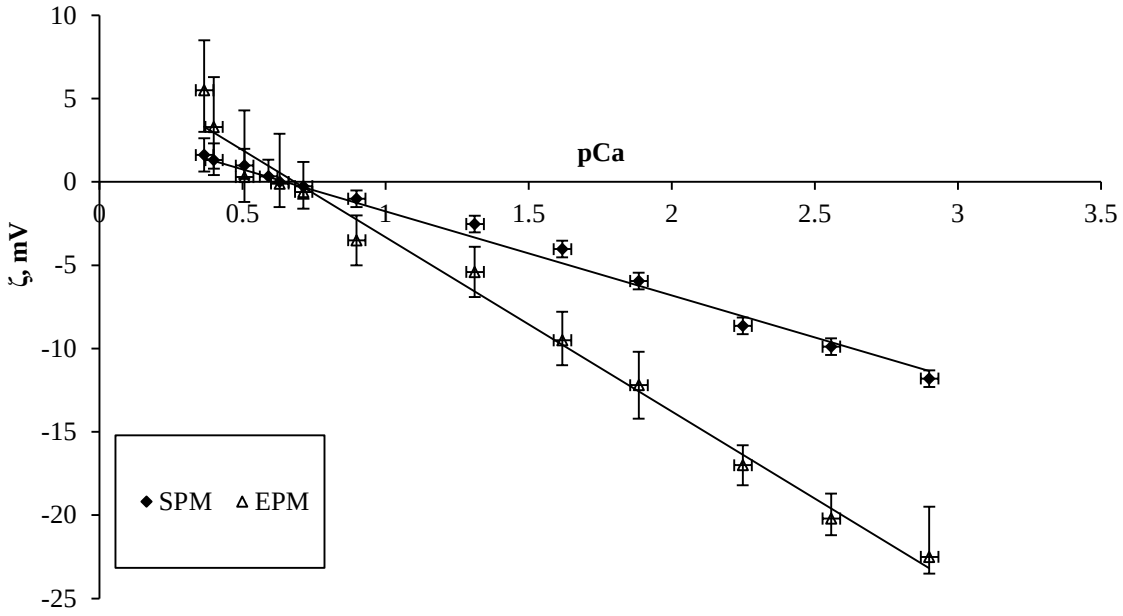

Figure 10. Comparison between zeta potential as a function of pCa obtained using the SPM and EPM method for the same natural Portland limestone and 0.05M NaCl electrolyte, pH = 7.2-8±0.3.

Table 4. Compilation of reported IEP values, including the electrolyte, type of calcite, pCa and whether the IEP was directly measured or extrapolated.

Reference	Background Electrolyte	Calcite	IEP, pCa	Determination
Somasundaran and Agar (1967)	DIW	Synthetic	3.72	extrapolated
Fuerstenau et al. (1968)	10^{-3}M (SiO_2/Na_2O)	Synthetic	4.1	extrapolated
Mishra (1978)	$2x10^{-3}$M $NaClO_4$	Natural	3.09	extrapolated
Foxall et al. (1979)	0.01-.15M NaCl	Synthetic	4.4	extrapolated
Amankonah and Somasundaran (1985)	$2x10^{-3}$M KNO_3	Synthetic	4.08	extrapolated
Thompson and Pownall (1989)	$2x10^{-3}$-10^{-2}M (NaCl/HCl/NaOH)	Synthetic	2.02	direct
Thompson and Pownall (1989)	$2x10^{-3}$-10^{-2}M (NaCl/$NaHCO_3$/HCl /NaOH)	Synthetic	1.92	direct
Thompson and Pownall (1989)	$2x10^{-3}$-10^{-2}M (NaCl/$CaCl_2$/HCl/N aOH)	Synthetic	2.16	direct
Thompson and Pownall (1989)	$2x10^{-3}$-10^{-2}M (NaCl/$CaCl_2$/HCl/N aOH)	Synthetic	3.4	direct

Thompson and Pownall (1989)	$2x10^{-3}$-10^{-2}M ($NaCl/H_2CO_3$)	Synthetic	4	direct
Thompson and Pownall (1989)	$2x10^{-3}$-10^{-2}M (NaCl/NaHCO3/H_2CO_3)	Synthetic	3.8	direct
Thompson and Pownall (1989)	$2x10^{-3}$-10^{-2}M (NaCl/NaHCO3/Ca$(OH)_2$)	Synthetic	3.8	direct
Pierre et al. (1990)	10^{-2}M NaCl	Synthetic	3.37	direct
Pierre et al. (1990)	10^{-3}-10^{-1}M NaCl	Natural	4	direct
Pierre et al. (1990)	0.03M NaCl (constant pH=8.3)	Natural	2	direct
Pierre et al. (1990)	10^{-2}M NaCl (constant pH=8.5)	Synthetic	3.9	direct
Huang et al. (1991)	DIW	Synthetic	4.35	extrapolated
Cicerone et al. (1992)	0.03M KCl	Synthetic	2.7	direct
Chen et al. (2014)	DIW	Natural	0.2-0.48	extrapolated

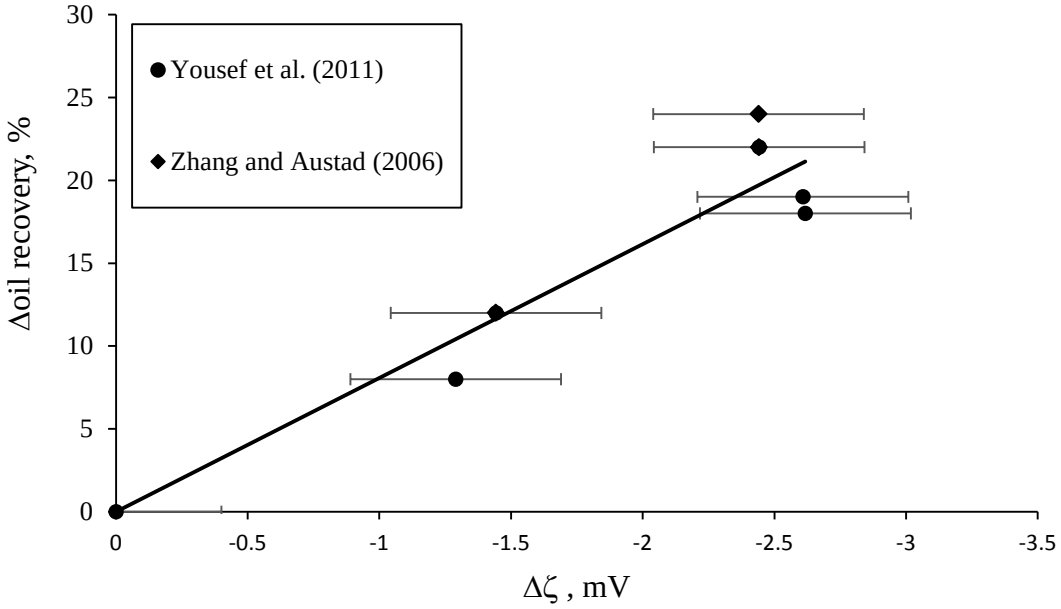

Figure 11. Comparison of the change in incremental oil recovery and zeta potential referenced to that of seawater for both controlled salinity (CSW) approaches: seawater dilution (Yousef et al, 2011) and sulfate addition to seawater (Zhang and Austad, 2006).